arXiv:0907.4746v2 [hep-ph] 16 Sep 2009

Nonabelian dark matter: models and constraints

Fang Chen, James M. Cline, Andrew R. Frey
Physics Department, McGill University, 3600 University Street, Montréal, Québec, Canada H3A 2T8
e-mail: fangchen, jcline, frey @physics.mcgill.ca
(Dated: July 2009)

Numerous experimental anomalies hint at the existence of a dark matter (DM) multiplet χ_i with small mass splittings. We survey the simplest such models which arise from DM in the low representations of a new SU(2) gauge symmetry, whose gauge bosons have a small mass $\mu \lesssim 1$ GeV. We identify preferred parameters $M_\chi \cong 1$ TeV, $\mu \sim 100$ MeV, $\alpha_g \sim 0.04$ and the $\chi\chi \to 4e$ annihilation channel, for explaining PAMELA, Fermi, and INTEGRAL/SPI lepton excesses, while remaining consistent with constraints from relic density, diffuse gamma rays and the CMB. This consistency is strengthened if DM annihilations occur mainly in subhalos, while excitations (relevant to the excited DM proposal to explain the 511 keV excess) occur in the galactic center (GC), due to higher velocity dispersions in the GC, induced by baryons. We derive new constraints and predictions which are generic to these models. Notably, decays of excited DM states $\chi' \to \chi\gamma$ arise at one loop and could provide a new signal for INTEGRAL/SPI; big bang nucleosynthesis (BBN) constraints on the density of dark SU(2) gauge bosons imply a *lower* bound on the mixing parameter ϵ between the SU(2) gauge bosons and photon. These considerations rule out the possibility of the gauge bosons that decay into e^+e^- being long-lived. We study in detail models of doublet, triplet and quintuplet DM, showing that both normal and inverted mass hierarchies can occur, with mass splittings that can be parametrically smaller (*e.g.,* $O(100)$ keV) than the generic MeV scale of splittings. A systematic treatment of Z_2 symmetry which insures the stability of the intermediate DM state is given for cases with inverted mass hierarchy, of interest for boosting the 511 keV signal from the excited dark matter mechanism.

PACS numbers: 98.80.Cq, 98.70.Rc, 95.35.+d, 12.60Cn

I. INTRODUCTION

In the last year, it was intriguingly suggested that a variety of observed astrophysical anomalies might be tied together by a single theoretical framework, in which transitions between states in a dark matter (DM) multiplet, mediated by new GeV-scale gauge bosons, could lead to production of lepton pairs [1]. These could explain excess electron/positrons seen by the PAMELA [2], ATIC [3], PPB-BETS [4], HEAT [5] and INTEGRAL/SPI [6] experiments (the latter via the excited DM proposal (XDM) [7]). In addition, it has been proposed that such transitions could account for the DAMA/LIBRA annual modulation [8] via the inelastic DM mechanism (iDM) [9]. Synchrotron radiation from the leptons could explain the WMAP haze [10]. More recently Fermi/LAT [11] and HESS [12] have made higher precision measurements of the e^+e^- spectrum at TeV energies, confirming an excess above the known background, although less pronounced than the ATIC data. The DM explanation for this excess has by now been studied by numerous authors [13, 14, 15, 16, 17, 18, 19, 20, 21, 22, 23, 24, 25, 26], and a plethora of models has been proposed [27], including ones where the DM decays rather than annihilates [28]. Pulsars provide a more conventional astrophysical explanation[1] for many of these anomalies, but the data do not yet clearly prefer them over the DM hypothesis [31]. However, constraints from secondary gamma rays produced by the charged leptons (or from primary neutrinos) are rapidly closing up the allowed DM parameter space [32, 33, 34, 35, 36, 37, 38, 39, 40, 41, 42, 43, 44, 45, 46, 47, 48]. Anticipated new data from the Fermi telescope is expected to tighten these constraints in the near future.

The theoretical paradigm we focus on here assumes that the DM transforms nontrivially under a nonabelian gauge symmetry which is spontaneously broken below the 10 GeV scale. Radiative corrections from virtual gauge bosons induce mass splittings between the DM states of order $\alpha_g\mu$, where $\alpha_g = g^2/4\pi$ is the fine structure constant of the new gauge symmetry and $\mu \sim gv$ is a characteristic gauge boson mass after spontaneous symmetry breaking. Multiple exchanges of the light gauge (or Higgs) bosons gives a Sommerfeld enhancement [1, 49] which can explain the large annihilation cross section needed in the galaxy, compared to the smaller one in the early universe at the DM freeze-out temperature, expected from the relic density. In our previous paper [50], we presented an SU(2) model along these lines which was designed to more easily give a large enough 511 keV signal as observed by INTEGRAL while also accommodating the PAMELA/ATIC observations.

Our goal in the present paper is to give a more comprehensive survey of models based on SU(2) gauge symmetry, considering a few different possibilities for the means of coupling the DM to the standard model, for the representation of the DM multiplet, and that of the scalars which break the gauge symmetry. We also derive some new constraints on the gauge and Higgs couplings which are particular to this class of models. We start by discussing a number of general issues which transcend the individual models.

---

[1] An even more conservative interpretation is that no new source is needed to fit the data; see for example ref. [29], or concerning the 511 keV excess, ref. [30]

The paper is organized as follows. Section II details the mechanism of kinetic mixing of dark and standard model (SM) gauge bosons, including its possible UV origin, and we derive a new constraint on the gauge coupling from the induced DM transition magnetic moment in the nonabelian case. Section III discusses the alternative of communication between the dark and SM sectors by Higgs mixing. We derive new constraints on diagonal Yukawa couplings of the dark Higgs to DM, from direct detection and from antiproton production in the galaxy. In section IV we discuss the concept of an inverted DM mass hierarchy for boosting the predicted 511 keV INTEGRAL signal, and the Z_2 symmetry and nonthermal DM history needed to make this idea work. Section V analyzes which regions of parameter space best fit the experimental anomalies (we do not insist on explaining DAMA, since the constraints on the iDM mechanism have become so severe [51, 52],[53]) and constraints from diffuse gamma rays, relic density, big bang nucleosynthesis, and laboratory constraints.

In the remainder of the paper we discuss several specific kinds of models, organized according to the SU(2) representation of the DM. Sections VI, VII and VIII respectively deal with DM in the doublet, triplet and quintuplet representations. In all of these models the gauge group is simply SU(2). For completeness and contrast, in section IX we consider one model with dark gauge group SU(2)×U(1) and triplet DM, which illustrates the differences between the purely nonabelian models and ones where gauge kinetic mixing occurs between U(1) field strengths. We summarize our findings in X. Appendices A and B respectively give details of the transition magnetic moment and radiative mass computations, C computes the annihilation cross sections for freeze-out of DM in a general representation, and E treats the diagonalization of the gauge boson and DM mass matrices for the SU(2)×U(1) model.

II. KINETIC MIXING OF GAUGE BOSONS

A simple way of generating couplings between one of the SU(2) gauge bosons and electrons is through nonrenormalizable couplings of the form

$$\sum_i \frac{1}{\Lambda_i} Y_{\mu\nu} B_a^{\mu\nu} \Delta_i^a \tag{1}$$

or

$$\sum_i \frac{1}{\Lambda_i^2} Y_{\mu\nu} B_a^{\mu\nu} h_i^\dagger \tau_a h_i \tag{2}$$

where Δ_a and h are respectively triplet and doublet Higgs fields which are assumed to get a VEV. By having several triplet or doublet fields (labeled by index i) which get VEV's in different directions, it is possible to get mixing with several colors of the B gauge boson. In (1), note that only a single linear combination of B vectors mixes with the SM. With a generic Higgs potential, we can always choose the linear combination of triplets in (1) to be Δ_1. However, depending on the Higgs potential, the vector that mixes with the SM may be a linear combination of several B mass eigenstates.

To understand the consequences of gauge boson mixing, it is useful to start with a simple example in which a massive abelian boson B mixes with the photon. The kinetic term is

$$-\frac{1}{4}\left(F_{\mu\nu}F^{\mu\nu} + B_{\mu\nu}B^{\mu\nu} - 2\epsilon B_{\mu\nu}F^{\mu\nu}\right) + \frac{1}{2}\mu^2 B_\alpha B^\alpha \tag{3}$$

Since the U(1) gauge symmetry of the photon is unbroken, it must remain strictly massless. This restricts the form of the transformation which diagonalizes the kinetic term to

$$A_\mu = \tilde{A}_\mu + \epsilon \tilde{B}_\mu \tag{4}$$

Therefore all particles which couple to the photon acquire a coupling of strength ϵe to the massive B gauge boson.

For the models we consider, the mixing takes the form $\frac{1}{2}\epsilon Y_{\mu\nu} B_1^{\mu\nu}$, where for concreteness we take color 1 of the nonabelian gauge boson to mix with the standard model weak hypercharge, it is straightforward to show that eq. (4) generalizes to the similar form

$$A^\mu = \tilde{A}^\mu + \epsilon \cos\theta_W \tilde{B}_1^\mu \tag{5}$$

where θ_W is the Weinberg angle. One must further transform B_1 and the Z gauge boson as

$$\begin{aligned} B_1^\mu &= \left[\tilde{B}_1^\mu - \epsilon \sin\theta_W \left(\frac{m_Z^2}{m_Z^2-\mu^2}\right) \tilde{Z}^\mu\right]\left(1 + O(\epsilon^2)\right) & (6)\\ Z^\mu &= \left[\tilde{Z}^\mu + \epsilon \sin\theta_W \left(\frac{\mu^2}{m_Z^2-\mu^2}\right) \tilde{B}_1^\mu\right]\left(1 + O(\epsilon^2)\right) & (7)\end{aligned}$$

where the tilded fields are those which diagonalize the kinetic term. Therefore the B_1 gauge boson acquires a coupling to the current of the Z boson, in addition to that of the photon. Figure 1(a) shows an example of a $\chi \to \chi' f\bar{f}$ transition mediated by the B_1.

The mass of the Z gets shifted by a fractional amount

$$\frac{\delta m_Z}{m_Z} = \epsilon^2 \sin^2\theta_W \frac{\mu^2}{2m_Z^2} \tag{8}$$

relative to its usual value. For the small values of $\epsilon \sim 10^{-3} - 10^{-4}$ and $\mu \lesssim$ GeV which are of interest, this is a negligible shift.

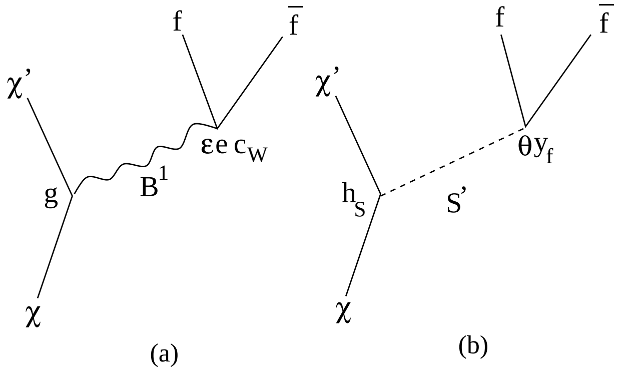

FIG. 1: Feynman diagrams for (a) $\chi \to \chi' f \bar{f}$ via gauge boson mixing (left) or (b) Higgs mixing (right).

With gauge boson mixing, the annihilation $\chi\chi \to B_1 B_1$ results in subsequent decays of $B_1 \to l^+ l^-$ with roughly equal branching ratios for all leptons l with mass below μ. Due to the nondiagonal couplings of B_1 to the χ states, assuming they are Majorana, there is no s-channel annihilation through a single virtual B_1. Hence the annihilation into 4 leptons is guaranteed. For Dirac DM, such as in the doublet representation, this need not be the case, as we will discuss in section VI.

A. Microscopic origin of gauge kinetic mixing

The dimension-5 operator (1) can be induced at one loop by a heavy particle X which carries both dark $SU(2)$ charge and weak hypercharge y_X, if it also has a Yukawa coupling to the dark sector Higgs triplet. Suppose X is a Dirac fermion which transforms as doublet of the SU(2), so the Yukawa interaction is

$$h_X \overline{X}_i (\tau_a)^i_j X^j \Delta^a \tag{9}$$

The diagram is shown in figure 2(a). It generates the effective interaction which can be estimated as

$$\frac{h_X\, y_X\, g}{16\pi^2 M_X} Y_{\mu\nu} B^{\mu\nu}_a \Delta_a \tag{10}$$

so that the mixing parameter is given by $\epsilon \cong h_X y_X g \Delta/(16\pi^2 M_X)$, where Δ is the VEV of the triplet Higgs. For couplings of order unity and $\Delta \sim 10$ GeV, M_X can be of order TeV to generate $\epsilon \sim 10^{-4}$.

Similarly, the dimension-6 operator (2) can arise from a heavy doublet scalar field S_i with a coupling $\lambda\, (S^\dagger \tau_a S)\, (h^\dagger \tau_a h)$ to another dark higgs doublet h (or perhaps the same one, $h \to S$). If S has weak hypercharge y_S, the analogous diagram with X replaced by S gives rise to the operator (2) with $\Lambda^2 \cong 16\pi^2 M_S^2/(g\lambda y_S)$.

B. Long-lived dark gauge bosons

It is noteworthy that pure SU(2) models generically predict small gauge mixing parameters ϵ, suppressed by powers of a heavy scale, whereas models with SU(2)×U(1) gauge symmetry in the dark sector allow for renormalizable mixing of SM and dark hypercharge, in which case there is no reason to expect particularly small values of ϵ. A phenomenological advantage of small ϵ is that values on the order of 10^{-16} give the gauge boson B_1 a lifetime of order 10^{12} s. Such a long lifetime lets B's produced from DM annihilation propagate away from the galactic center before decaying. This delocalizes gamma rays produced by the leptonic decay products, allowing such models to evade HESS constraints [20, 25]. However we will show in section V E that gauge bosons with a lifetime greater than ~ 1 s are ruled out by big bang nucleosynthesis for the models considered in this work.

C. Direct decay of excited DM to photon

Because there is no mixing of B_1^μ to $\tilde{A}^\mu$ in eq. (6), there is no tree level amplitude for the decay of excited DM directly to a photon. For example in the case of triplet DM, one would have the decay $\chi_3 \to \chi_2 \gamma$ if such a mixing existed. Instead the dominant decay is $\chi_3 \to \chi_2 l^+ l^-$ mediated by the B_1. However, in the class of models with kinetic mixing between SM hypercharge and one of the dark SU(2) gauge bosons, it is inevitable for the single photon final state to arise at the loop level, as we now show. Naively, one could draw the diagram where $l^+ l^-$ form a loop connecting B_1 to the photon, but this just renormalizes the kinetic mixing term, so it is not relevant. There is another process which occurs due to the nonabelian nature of the B_1, illustrated in fig. 2(b).

The novel feature of the gauge mixing operator is that $B_1^{\mu\nu}$ contains the term $g(B_2^\mu B_3^\nu - B_2^\nu B_3^\mu)$. There is thus a trilinear vertex coupling these gauge bosons to the weak hypercharge field strength, with strength ϵg. One consequence of this interaction is the generation of a transition magnetic moment for the DM. An example is shown in fig. 2(b) for the case of DM in the triplet representation. A magnetic moment interaction of the form $\mu_{23} \bar{\chi}_2 \sigma_{\mu\nu} \chi_3 F^{\mu\nu}$ arises, where μ_{23} is expected to be of order $\epsilon g^3/(16\pi^2 M_\chi)$. A careful computation of the loop

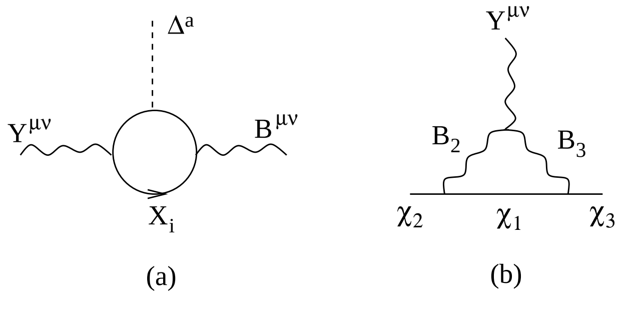

FIG. 2: Loop diagrams which generate (a) gauge kinetic mixing (left) and (b) DM transition magnetic moment (right).

diagram given in appendix A gives

$$\mu_{23} \cong \frac{\epsilon g^3 c_W}{128\pi^2 M_\chi}\left(\ln\frac{M_\chi}{\mu} - 1\right) \tag{11}$$

where μ is the scale of the nonabelian gauge boson masses and $c_W = \cos\theta_W$. It is straightforward to compute the rate Γ_γ for $\chi_2 \to \chi_3\gamma$,

$$\Gamma_\gamma = \frac{\mu_{23}^2}{8\pi}(\delta M_{23})^3 \tag{12}$$

where $\delta M_{23} = M_{\chi_2} - M_{\chi_3}$ is the energy available for the decay. On the other hand, the rate Γ_{2e} for $\chi_2 \to \chi_3 e^+e^-$ is approximately $(\delta M_{23}-2m_e)^2(\delta M_{23}+2m_e)/(256\pi^3 M_\chi^2)$ times the spin-averaged squared matrix element,

$$\langle|\mathcal{M}|^2\rangle \cong 32 g^2 e^2 \epsilon^2 c_W^2 \frac{M_\chi^2}{\mu^4}\left(E_+E_- + \vec{p}_+\cdot\vec{p}_- - m_e^2\right) \tag{13}$$

(where $E_\mp$ and $\vec{p}_\mp$ are the energy and 3-momenta of the electron and positron, respectively). This varies approximately linearly over the allowed phase space, so we estimate the integral as being

$$\Gamma_{2e} \cong 4\epsilon^2\alpha\alpha_g(\delta M_{23} - 2m_e)^3(\delta M_{23} + 2m_e)^2/\mu^4 \tag{14}$$

The branching ratio for the single photon versus the two lepton decay is thus

$$\mathrm{BR}_\gamma = \frac{c_W^2\,\alpha_g^2/\alpha}{8192\pi^2}\,\frac{\mu^4(\delta M_{23})^3}{M_\chi^2(\delta M_{23-})^3(\delta M_{23+})^2}\,\ln^2\frac{M_\chi}{e\mu} \tag{15}$$

where $\delta M_{23\pm} = \delta M_{23} \pm 2m_e$ and $e = 2.71828\dots$. Taking $\delta M_{23+} \cong 2\delta M_{23} \cong 4m_e$ but allowing for the possibility that $\delta M_{23-} \ll \delta M_{23}$, we can write

$$\begin{aligned}\mathrm{BR}_\gamma \;&\cong\; 2.6\times 10^{-4}\,\frac{\alpha_g^2}{\alpha}\left(\frac{\mu}{200\text{ MeV}}\right)^4\left(\frac{1\text{ TeV}}{M_\chi}\right)^2\\ &\times\left(\frac{100\text{ keV}}{\delta M_{23-}}\right)^3\end{aligned} \tag{16}$$

The reference values chosen here are compatible with constraints which we will discuss in later sections, and small values of δM_{23-} enhance the size of BR_γ.

Even though the branching ratio for $\chi_3 \to \chi_2\gamma$ due to the magnetic moment is small, the observable signal due to this process, in the diffuse gamma ray background, is distinctive. If the dark matter was at rest, it would produce a monoenergetic photon with $E = \delta M \sim$ MeV. Since the central galactic DM has a velocity distribution with dispersion $v/c \sim 10^{-3}$, the spectrum of the photon is Doppler broadened with a width of order $(v/c)\delta M \sim 1$ keV for $\delta M_\chi \sim$ MeV. This is just below the 1.5 keV resolution of SPI. The nonobservation of such a signal by INTEGRAL thus provides a new constraint on models with S-parameter type mixing of the nonabelian gauge boson with weak hypercharge.

To determine the constraint, we can compare the new direct photon signal with that of the 511 keV line already observed by INTEGRAL. The latter is seen with a confidence level (c.l.) of 50σ and a signal to background ratio (S/B) of a few percent. One can predict the c.l. of the new signal from that of the 511 keV line through the relation

$$(\text{c.l.})_{\text{new}} = (\text{c.l.})_{511}\,\mathrm{BR}_\gamma\,\frac{(S/B)_{\text{new}}}{(S/B)_{511}}\left(\frac{\sigma_{511}}{\sigma_{\text{new}}}\right)^{1/2} \tag{17}$$

where $\sigma_{511} \cong 5$ keV is the width of the 511 keV line and $\sigma_{\text{new}} = 1.5$ keV is the resolution of the detector (which is approximately the same as the intrinsic line width). To understand the dependence on width, notice that for fixed flux, increasing the width of a line reduces the signal proportionally $(1/\sigma)$, but for fixed signal-to-background, it increases the counting statistics by $\sqrt{\sigma}$ since a wide line of a given intensity has more flux than a narrow one. These effects combine to give the $1/\sqrt{\sigma}$ dependence. The background for the 511 keV line is dominated by the positronium $\to 3\gamma$ continuum and annihilations of positrons in the INTEGRAL telescope, effects which are both absent for the new signal. On the other hand, there is a broad instrumental line near 1.8 MeV which is the dominant background for the narrow galactic ^{26}Al line [54], whose signal to background ratio is around 70/30. Putting these numbers together, and assuming that $(\text{c.l.})_{\text{new}} < 3$ to avoid a detection, we find the limit

$$\alpha_g \lesssim 0.08\left(\frac{200\text{ MeV}}{\mu}\right)^2\left(\frac{M_\chi}{1\text{ TeV}}\right)\left(\frac{\delta M_{23-}}{100\text{ keV}}\right)^{3/2} \tag{18}$$

(recall that $\delta M_{23-} = \delta M_{23} - 2m_e$). It is interesting that such reasonable values of the dark gauge coupling could lead to an additional signal potentially detectable by INTEGRAL. However, it would require a nonthermal DM history, since we will show that smaller values of α_g are needed for the correct relic density, eq. (36), or in the case of doublet dark matter, the bound (18) does not apply because the magnetic moment is suppressed by an additional factor of $\delta M_{23}/M_\chi \sim 10^{-6}$, as we will show in section VI A.

III. MIXING THROUGH THE HIGGS SECTOR

A. General features

An alternative way in which the dark matter might couple to the standard model is through renormalizable operators of the form

$$\lambda_{HS}|H|^2|S|^2 \tag{19}$$

where H is the standard model Higgs doublet and S is a Higgs field which is charged under the dark SU(2) gauge group. If S gets a VEV $v_S/\sqrt{2}$ and also has a Yukawa coupling to the DM, schematically of the form $h_s S\chi\chi$, then transitions such as $\chi \to \chi f\bar{f}$ can be mediated by the Higgs bosons as shown in figure 1(b). The Higgs sector has a mass matrix of the form

$$\begin{pmatrix} m_H^2 & \lambda_{HS} v_H v_S \\ \lambda_{HS} v_H v_S & m_S^2 \end{pmatrix} \tag{20}$$

where v_H is the VEV of the SM Higgs $h = \sqrt{2}H$. If the mixing is small, then the Lagrangian fields are related to the mass eigenstates by

$$\begin{pmatrix} H \\ S \end{pmatrix} \cong \begin{pmatrix} 1 & -\theta \\ \theta & 1 \end{pmatrix} \begin{pmatrix} H' \\ S' \end{pmatrix}, \quad \theta = \frac{\lambda_{HS} v_H v_S}{m_H^2 - m_S^2} \tag{21}$$

Therefore S' couples with strength $y_f\theta$ to any SM model fermion f whose Yukawa coupling to H is y_f. In addition, the H' couples to $\chi\chi$ with strength $-y_S\theta$. Thus the diagram involving H' exchange is of the same order in couplings as that with the S', but at low momentum transfer it is suppressed by m_S^2/m_H^2.

B. Constraints on diagonal couplings

1. No antiproton production

An interesting qualitative difference between Higgs and gauge boson mixing is that in the former case, the Yukawa couplings are generally not off-diagonal. For example, triplet dark matter coupling to a quintuplet scalar as $\chi^a S_{ab}\chi^b$ has diagonal couplings; similarly for doublet dark matter coupling to a triplet scalar via $\chi_i\tau^a_{ij}\chi_j S_a$. In either case, the annihilation $\chi\chi \to S \to f^+f^-$ shown in fig. 3(a) occurs, resulting in quark or lepton pairs favoring the most strongly coupled fermions—the top quark. To avoid production of hadrons, since no antiproton excess is observed by PAMELA, one needs to have mixing with a scalar that has dominantly off-diagonal couplings so that $\chi_1\chi_1$ annihilates primarily to a pair of S bosons by virtual χ_2 exchange. The S bosons decay nearly on shell and hadron production can be suppressed if the S is lighter than $\sim$ 1 GeV. Note that it is impossible to keep the couplings strictly off-diagonal in the mass basis, once the relevant component of S gets a VEV, since this contributes an off-diagonal mass term to the DM. Therefore the Higgs mixing scenario in its simplest form could be disfavored by the lack of any antiproton excess in the PAMELA data.

Moreover, diagonal couplings are constrained by direct dark matter searches, by the process shown in fig. 3(b). Translating the limit quoted in eq. (11) of ref. [1] to the present case (and assuming $m_S = 200$ MeV), a diagonal Yukawa coupling h_s is bounded by

$$\theta h_s y_N < 16\pi \times 10^{-8}\alpha_{\rm em} \;\Rightarrow\; \theta h_s < 4\times 10^{-6} \tag{22}$$

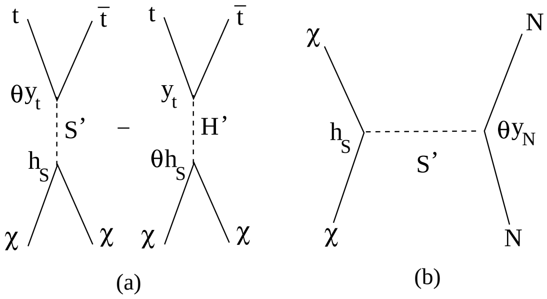

FIG. 3: (a) Left: DM annihilation into t-$\bar{t}$ by virtual scalar that mixes with Higgs. (b) Right: DM scattering on nucleon by scalar exchange.

Here $y_N \cong 10^{-3}$ is the Higgs-nucleon coupling [55]. Assuming that the SM Higgs mass m_H is much heavier than m_S, this implies

$$h_s\lambda_{HS} < 2.7\times10^{-4}\left(\frac{m_S}{200\text{ MeV}}\right)^2\left(\frac{m_H}{130\text{ GeV}}\right)^2\left(\frac{1\text{ GeV}}{v_S}\right) \tag{23}$$

To illustrate how severe (or mild) this constraint might be, consider the case of triplet DM χ_a coupled to a quintuplet (traceless symmetric tensor) scalar S_{ab}, via $h_s\chi_a S_{ab}\chi_b$, and the cross-coupling $\lambda H^2\,{\rm tr}S^2$ to the SM Higgs H. Suppose for example that S_{12} gets a VEV $S \sim 1 - 10$ GeV to induce mixing with H, with mixing angle $\theta \cong \lambda_{HS} S v_H/m_H^2$. In addition to radiatively generated mass splittings of the DM (as we will discuss below), there is a tree level contribution $h_s S\chi_1\chi_2$ so that the mass eigenstates become linear combinations, $\chi_\pm = \sqrt{1/2}(\chi_1 \pm \chi_2)$. The fluctuations δS of S_{12} thus couple to the mass eigenstates as $h_s\delta S(\chi_+^2 - \chi_-^2)$. Therefore the ground state χ_- can annihilate directly into a single fermion pair through a single intermediate scalar. The latter is always far off shell, so this annihilation channel is dominated by production of top quarks which hadronize and produce antiprotons, contrary to the observations. However notice that the two diagrams in fig. 3(a) interfere destructively. We can estimate the effect of these diagrams by integrating out the intermediate scalar, and using the fact that $m_S \ll m_H$, to get the effective dimension-6 operator

$$\theta y_t h_s \frac{m_H^2}{M^4}\,\chi\chi\,\bar{t}t \tag{24}$$

On the other hand, the annihilation $\chi\chi \to S'S'$ by χ exchange can be estimated from the dimension-5 operator

$$\frac{h_s^2}{M_\chi}\chi\chi S'^2 \tag{25}$$

Assuming that the initial χ's are nonrelativistic, the ratio of the corresponding cross sections is of order

$$\frac{\sigma(\chi\chi \to \bar{t}t)}{\sigma(\chi\chi \to S'S')} \sim \frac{\theta^2 y_t^2}{h_s^2}\,\frac{m_H^4}{M_\chi^4} \tag{26}$$

The top quarks decay to b quarks before hadronization, and each b quark produces $\sim$ 4.5 antiprotons (using

MicrOMEGAs [56]), so the number of antiprotons per positron is of the same order. The observed flux of antiprotons to electrons is approximately 10^{-3}, and given that no antiprotons in excess of standard expectations are observed, we should demand that the ratio (26) not exceed this limit. For definiteness, if $M = 1$ TeV we obtain the rather weak constraint

$$\lambda_{HS} \lesssim 85\, h_S \left(\frac{M_\chi}{1\text{ TeV}}\right)\left(\frac{1\text{ GeV}}{v_S}\right) \tag{27}$$

Both (27) and the direct detection constraint (23) can be satisfied using reasonable values of the couplings.

Furthermore, if there are additional contributions to the DM mass splittings, it is possible to parametrically suppress the diagonal couplings. For example, consider a second quintuplet Higgs T_{ab} with coupling $h_T\chi_a T_{ab}\chi_b$, and a VEV which splits the χ masses diagonally, $h_T T(\chi_1\chi_1 - \chi_2\chi_2)$. In this case, the χ mass eigenstates are not maximal mixtures of the flavor states; rather $\chi_+ = \chi_1 + \delta\chi_2$, $\chi_- = \chi_2 - \delta\chi_1$, with $\delta = h_S S/h_T T$ (assuming δ is small). If the $|T|^2|H|^2$ coupling is negligible, then the overall effect is to reduce the diagonal couplings by the factor δ, while leaving the off-diagonal couplings unsuppressed.

The constraint due to the assumed lack of production of antiprotons would be weakened even further if the recent claim of ref. [57] is verified. This work questions the assumption that the observed antiproton background is actually understood in terms of physics other than dark matter annihilation.

2. *No two-lepton final states*

In section V D we will discuss the fact that recent constraints on DM annihilation from the diffuse gamma ray background are more severe for models in which $\chi\chi \to 2l$ than $4l$ final states (where l is a charged lepton) due to the harder spectrum in two-body decays. This is not an issue when the intermediate particle is an SU(2) gauge boson, since its couplings are automatically off-diagonal and thus two bosons must be emitted in the annihilation, but it might be an issue for intermediate Higgs bosons with diagonal couplings. However, the result (26) can be directly adapted to the case of decays to a lepton pair instead of a top pair by substituting the lepton Yukawa coupling for that of the top. Even for the heaviest lepton, τ, the result is suppressed by $(y_\tau/y_t)^2 \cong 10^{-4}$. These annihilations are thus much more rare than those with the $\bar{t}t$ final states, and do not provide a stronger constraint than the one derived above, even if we only demand that the ratio be $\ll 1$ rather than $\lesssim 10^{-3}$.

C. Long-lived dark Higgs boson

In order to realize the long-lived intermediate state proposal of ref. [20], it is interesting to know how small a mixing angle is required to get the Higgs lifetime to be 10^{12} s. In section V it will be aruged that Higgs masses in the range mass $m_S \lesssim 100$ MeV are the most promising for fitting PAMELA/Fermi observations, such that only the e^+e^- final state is available. Using the decay rate $\Gamma \cong \theta^2 y_e^2 m_S/16\pi$, we find that

$$\theta = 6\times 10^{-12}\left(\frac{100\text{ MeV}}{m_S}\right)^{1/2} \tag{28}$$

is the required value. We will show in section V E 3 that such small values are strongly excluded by constraints on the density of dark gauge bosons, which must decay before BBN.

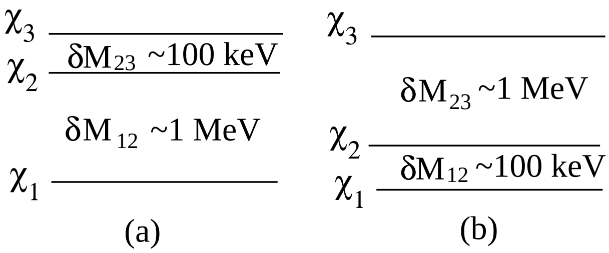

FIG. 4: (a) Left: inverted mass hierarchy of triplet DM; (b) Right: normal hierarchy.

IV. INVERTED MASS HIERARCHY AND Z_2 SYMMETRY

In the following models, a recurring theme will be whether it is possible to have a stable excited DM state which is slightly lighter than the highest excited state (the one that decays into leptons plus ground state). This "inverted hierarchy" is shown in figure 4(a), in contrast to the "normal hierarchy," fig. 4(b). We proposed the inverted hierarchy in ref. [50] as a means of boosting the galactic 511 keV signal from excited dark matter, since the transition $\chi_2\chi_2 \to \chi_3\chi_3$ requires less energy than $\chi_1\chi_1 \to \chi_3\chi_3$ and therefore benefits from a larger proportion of the DM velocity distribution.

A. Radiative mass corrections

Let us first review the mechanism of radiative mass splitting of a DM multiplet by virtual massive gauge bosons, through diagrams like that shown in fig. 5(a). Although the correction to the mass is logarithmically divergent, mass differences between members of the multiplet are finite. By choosing a suitable counterterm, the finite part which contributes to the mass splitting can be defined as

$$\delta M_i \cong -\frac{1}{2}\alpha_g \sum_j \mu_j T^j_{ia} T^j_{ai} \tag{29}$$

where $\alpha_g = g^2/4\pi$ and the sum runs over all the gauge bosons, with mass μ_j, which contribute in the intermediate state. The approximation (29) is valid when $\mu_j \ll M_\chi$. Details of the derivation are given in appendix B.

If Higgs mixing rather than gauge boson kinetic mixing is the dominant portal between the dark and SM sectors, it is likely that the dominant souce of mass splittings is the tree level contributions from the Higgs VEVs. It is possible however that the analogous radiative corrections with the intermediate Higgses, fig. 5(b), have an important effect. In appendix B it is shown that the analogous formula to (29) in this case is

$$\delta M_i \cong +\frac{1}{4}\alpha_y \sum_j m_j \tag{30}$$

where $y = \sqrt{4\pi\alpha_y}$ is the relevant Yukawa coupling for the Higgs multiplet in the loop, and m_j is the mass individual components of that multiplet.

B. Z_2 symmetry

The idea of exciting the intermediate state χ_2 depends on it being significantly populated and stable on cosmological time scales. One possibility is for it to be absolutely stable, which should be guaranteed by some symmetry. Another, which has been explored in ref. [58], is that the state is only metastable. In section V F we will discuss that this scenario is strongly constrained by direct detection considerations. In this paper we will highlight models that admit a discrete Z_2 parity, which not only ensures the stability of the intermediate state, but also forbids transitions between it and the neighboring states, that could be coupled to currents of SM particles.[2] The absence of these transitions makes the models safe from the direct detection constraints. (For other references discussing symmetries which stabilize DM, see [59].)

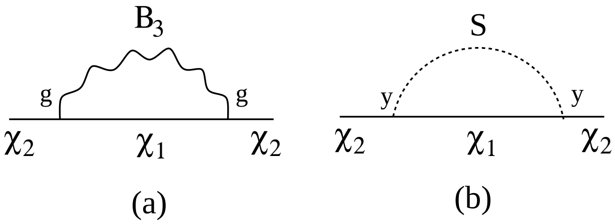

FIG. 5: Examples of radiative correction leading to mass splittings within DM multiplet from exchange of virtual gauge bosons (left) and Higgs bosons (right).

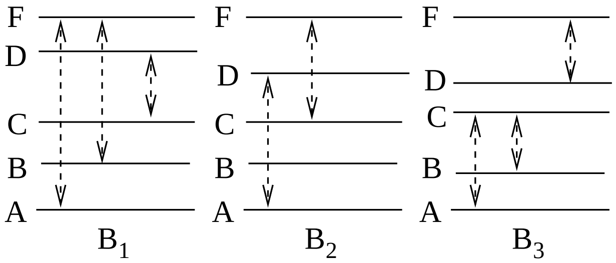

FIG. 6: Transitions between quintuplet states mediated by the three gauge bosons B_1, B_2, B_3.

The simplest example is triplet DM χ_i in which only one gauge boson color, say B_2, mixes with the SM hypercharge. In this case we can assign conserved Z_2 charges to the fields

$$\chi_1,\ \chi_3, B_1, B_3 \tag{31}$$

and to no others. Suppose that χ_1 is the ground state and χ_3 the heaviest state. Because of the Z_2 symmetry, χ_2 can never decay into χ_1 plus SM particles. It could in principle decay into $\chi_1 B_3$, but this is kinematically blocked by the mass of the B_3. From the point of view of the symmetry, there is no light particle that can appear in the final state to compensate the Z_2 charge of the χ_1.

Alternatively, we can state the condition that would make it impossible to keep the intermediate state stable. From the above argument we see that a necessary requirement is to be able to assign Z_2 charge to the ground state. Therefore the highest excited state of interest must also be charged. If any gauge boson which mediates transitions between the intermediate state and either of the charged states mixes with SM hypercharge, then Z_2 charges cannot be consistently assigned.

C. $Z_2 \times Z_2'$ symmetry for quintuplet DM

The issue of having a stable intermediate state does not arise for DM in the doublet representation, but it can be applied to higher representations, such as the symmetric tensor (quintuplet). We can label the canonically normalized states of χ_{ab} by

$$\langle\chi\rangle = \begin{pmatrix} A - B/\sqrt{3} & C & D \\ C & 2B/\sqrt{3} & F \\ D & F & -A - B/\sqrt{3} \end{pmatrix} \tag{32}$$

The transitions mediated between these states by the three B_i gauge bosons are shown in figure 6. Let us consider how to assign Z_2 charges to the states in a systematic way. First, suppose that one of the gauge bosons, say B_a, mixes with SM hypercharge. Then B_a must not carry Z_2 charge, while the other B's do; call these B_i. This implies that some subset X of χ's which appear only linearly and not bilinearly in the gauge interactions of the B_i's should also be charged. The states in X must also have the property that they only appearly bilinearly and not linearly in the interactions of B_a.

---

[2] Such transitions, if they exist, can always mediate decays $\chi_2 \to \chi_1 + 3\gamma$, as in fig. 17(a).

Using this logic, we can make an exhaustive list of the possible Z_2 charge assignments for a given choice of the B that mixes with hypercharge, which we denote by $B_a \leftrightarrow e^+e^-$. In the process, we discover that actually the global symmetry is larger than just Z_2; for a given subset X of χ states, its complement Y could also have been chosen. This means that we can assign Z_2 charge to states in X, and a separate Z_2' to states in Y. Meanwhile, the two gauge bosons other than B_a transform under both Z_2 and Z_2'. The result is

$$\begin{aligned} B_1 \leftrightarrow e^+e^- : &\quad X = \{C, D\},\ Y = \{A, B, F\} \\ B_2 \leftrightarrow e^+e^- : &\quad X = \{C, F\},\ Y = \{A, B, D\} \\ B_3 \leftrightarrow e^+e^- : &\quad X = \{D, F\},\ Y = \{A, B, C\} \end{aligned} \tag{33}$$

It turns out that the A and B states always mix to form the heaviest (A') and lightest (B') mass eigenstates. We therefore take the heaviest state relevant for the INTEGRAL transition to be one in Y, and this dictates that the intermediate state whose stability is to be guaranteed is the lightest one in X. The $Z_2 \times Z_2'$ symmetry then insures that the Z_2-charged intermediate state cannot decay into the Z_2'-charged lowest state, since both symmetries would be violated. We will give explicit examples in section VIII B 1.

In order for this to work, at least one of the Z_2's must be left unbroken by the VEVs of the Higgs fields. If there is only one triplet Higgs which gets a VEV to accomplish kinetic mixing, this presents no difficulty since then the Higgs components can transform in just the same way as the corresponding gauge fields, preserving both Z_2's. Moreover components of a quintuplet Higgs can be given the same charges as the corresponding DM components, so one Z_2 can be preserved as long as VEVs appear only in the X or Y subsets, but not both.

VEVs of additional doublets break all of the discrete symmetries, but multiple triplet VEVs can be consistent with the symmetries if they are orthogonal. Consider two triplets with VEVs $\vec{\Delta}$ and $\vec{\Delta}'$ in the 1 and 2 directions, respectively, and suppose that $\vec{\Delta}$ is used to generate kinetic mixing between B_1 and the SM. Then a single Z_2 is preserved, under which the fields B_2, B_3, Δ_2, Δ_3 and Δ_1' change sign, while Δ_1, Δ_2' and Δ_3' do not. Adding a third triplet Δ'' with VEV in the 3 direction is also consistent with the Z_2, if Δ_1'' transforms under it.

D. Nonthermal history

Even though Z_2 symmetry guarantees the stability of the intermediate state χ_2, it cannot prevent depletion of its density in the early universe, through exactly the same process needed for the INTEGRAL signal, namely $\chi_2\chi_2 \to \chi_3\chi_3$ followed by $\chi_3 \to e^+e^-\chi_1$ decay. Even more simply, the depletion could occur directly by $\chi_2\chi_2 \to \chi_1\chi_1$. In ref. [50], we noted that this depletion could be prevented if the χ's were produced out of thermal equilibrium rather than through the standard freeze-out. If the χ's are decay products of a supermassive scalar S, their initially high energies suppress the annihilation cross section sufficiently long to keep the $\chi_2\chi_2 \to \chi_3\chi_3$ excitation or the $\chi_2\chi_2 \to \chi_1\chi_1$ relaxation out of thermal equilibrium in the early universe.

In more detail, suppose that the gauge coupling α_g is too large to yield the right relic density from freeze-out. It was envisioned that S could decay at a low temperature ~ 5 MeV, resulting in mildly relativistic DM with momenta $p \sim 10^5 T$. The Sommerfeld enhancement is initially absent for DM with such large velocity, and in fact the rate of annihilations remains always less than the Hubble rate before cosmological structure begins to form, because $n\langle\sigma v\rangle$ and H both scale like T^2. Only when DM begins to concentrate in halos does the rate of annihilations become significant.

V. FITTING PAMELA/FERMI/HESS VERSUS INTEGRAL/SPI, COSMOLOGY AND LABORATORY BOUNDS

A. Fits to PAMELA/Fermi/HESS

Ref. [25] has identified regions in the parameter space of M_χ and $\sigma_{\rm ann}v_{\rm rel}$ for the process $\chi\chi \to BB$ (followed by $B \to e^+e^-$) which are compatible with the PAMELA/Fermi/HESS e^+e^- observations, as well as the HESS constraints on inverse Compton gamma rays produced by the electrons and positrons coming from DM annihilation.[3] As we will discuss in further detail below, additional constraints from extragalactic diffuse gamma ray production favor the models in which the B's from $\chi\chi$ annihilation decay only to e^+e^- and no heavier leptons. This implies that the mass of the B's, μ, must be less than twice the mass of the muon, $\mu \lesssim 200$ MeV. The allowed region for this scenario is reproduced in fig. 7. It should be emphasized that the two-body decay $\chi\chi \to e^+e^-$ mediated by a single B exchange is excluded because its electron spectrum ends too abruptly due to its near monoenergeticity [25]; this channel also provides a very poor fit to the PAMELA data [18]. Moreover in the class of models considered here, it would be impossible to forbid the channels $\chi\chi \to f\bar{f}$ where f is any SM fermion, if $\chi\chi \to e^+e^-$ is unsuppressed.

The best fit is in the vicinity of $\langle\sigma_{\rm ann}v_{\rm rel}\rangle \cong 10^{-23}$ cm^3/s and $M_\chi \cong 1$ TeV. This cross section exceeds that needed for the correct thermal relic density ($10^{-36} \cdot c$ cm^2 [60]) by a factor of $B = 330$, which is thus the required

---

[3] A recent analysis of preliminary Fermi observations of gamma rays from the inner galaxy is also consistent with this annihilation channel [47].

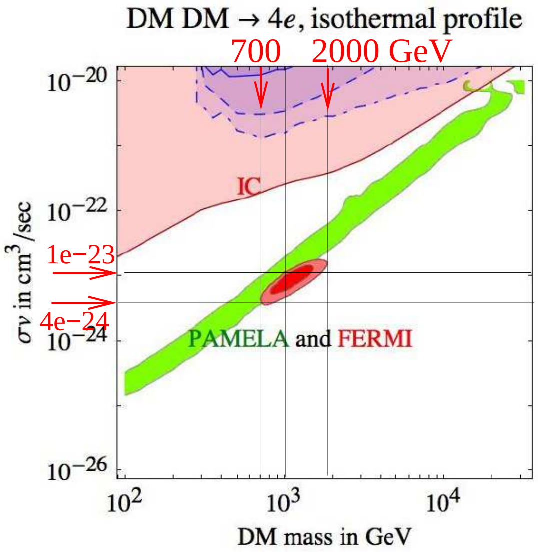

FIG. 7: Best fit of ref. [25] to the $\chi\chi \to 4e$ annihilation channel, in plane of $\langle\sigma v_{\rm rel}\rangle$ and M_χ. Shaded regions in upper part are excluded by diffuse gamma ray constraints.

boost factor, assuming a thermal origin for the DM. Even if a nonthermal origin is assumed, the thermal component should be suppressed by having an even larger cross section, and thus 330 should be regarded as an upper bound on the required boost factor.

The example shown assumes an isothermal radial density profile, which eases the constraints from HESS on the inverse Compton photons by lowering the DM density near the galactic ridge. For preferred profiles such as Einasto, the fit to PAMELA/Fermi is nearly ruled out. The isothermal profile is considered to be unrealistically flat near the center compared to the results of the best N-body simulations, but it was noted in [25] that long-lived intermediate bosons (the B gauge bosons in our case) could justify such an effective profile, due to the B's traveling away from the galactic center before decaying [20]. We will show that in section V E 1 below that big bang nucleosynthesis constraints rule out such a long-lived B in the present class of models, hence the mechanism of long-lived intermediate states cannot work here.

Another way of decentralizing the region of DM annihilation has been proposed in [1], however, which could have a quantitatively similar effect to the softer halo profile; namely DM subhalos which populate the halo could dominate as annihilation sites, due to their lower velocity dispersion and hence larger Sommerfeld enhancement. The small-velocity subhalo scenario has recently been studied in detail in ref. [45] (see also [61, 62, 63]), with reference to models favored by the pre-Fermi analysis of [18], in particular with $M_\chi = 1$ TeV, $\mu = 200$ MeV and $\alpha_g \cong 0.04$. This happens to be close to the preferred values mentioned above; we will show in the next section that this value of α_g is just slightly larger than the one needed to get the right relic density for triplet DM.

Still, to avoid the stronger inverse-Compton constraints on the preferred Einasto profile, it may be necessary to reduce the annihilation rate near $r = 0$, in addition to providing alternative subhalo regions for the annihilation. Recent work on halo formation including the effects of baryons indicates that the velocity profile steepens considerably (diverging like $r^{-1/4}$) for $r \lesssim 20$ kpc instead of leveling off to smaller values [64] as in pure DM simulations. (This reference also finds that the DM density profiles are softened near the center, a result not corroborated by other simulations which include baryons [65], but the latter work does qualitatively confirm the steepening of the velocity profile [66].) Moreover the overall magnitude of the velocity is somewhat increased for $r \lesssim 100$ kpc. Because the Sommerfeld enhancement of the annihilation cross section scales like $1/v$, this should have a similar effect to erasing the cusp of the density profile, making it more similar to the isothermal profile.

B. Relic density

We have computed the early-universe annihilation cross section of DM in any SU(2) representation into dark gauge bosons. For the three representations we focus on in this paper, the result is

$$\langle\sigma_{\rm ann} v_{\rm rel}\rangle \cong \frac{\pi\alpha_g^2}{M_\chi^2} \times \left\{ \begin{array}{ll} 0.14, & \text{doublet} \\ 0.88, & \text{triplet} \\ 5.18, & \text{quintuplet} \end{array} \right\} \qquad (34)$$

Details are given in appendix C. Using the standard value $\langle\sigma v_{\rm rel}\rangle = 10^{-36}$ cm$^2 \cdot c$ needed for thermal relic abundance [60], comparison with the cross section (34) indicates that the values of α_g required are

$$\alpha_g \;=\; \left\{ \begin{array}{ll} 0.077, & \text{doublet} \\ 0.031, & \text{triplet} \\ 0.013, & \text{quintuplet} \end{array} \right\} \times \left(\frac{M_\chi}{1\ \text{TeV}}\right) \qquad (35)$$
$$\text{(relic density value)}$$

As mentioned above, there are motivations to question the assumption that DM has a thermal origin, such as our inverted mass hierarchy proposal [50] (see also [58] and [67]). It is important to notice that to justify a nonthermal origin, the thermal contribution must be smaller than usual so that it is subdominant to the nonthermal contribution; thus the annihilation cross section would be larger. The values (36) should then be regarded as lower bounds.

These bounds can be evaded if the DM has stronger Yukawa couplings to dark Higgs fields; for example triplet DM can have the coupling $h\chi_i\Sigma_{ij}\chi_j$ to a quintuplet Higgs Σ. If $h \gg g$ then the freeze-out density is determined by h and the gauge coupling can be smaller than in (36). In such a case, it should be kept in mind that the annihilation in the galaxy will probably also be dominated by

Higgs boson exchange; notice that the mass scale of the Higgs bosons cannot naturally exceed that of the gauge bosons by a large factor, since the scale of spontaneous breaking of the dark SU(2) gauge symmetry is dictated by the mass scales in the Higgs sector. Thus late-time annihilations would likely be dominated by Sommerfeld-enhanced Higgs exchange diagrams. The expected boost factor would thus still be ~ 300 even in cases where α_g is much smaller than indicated in (36).

C. Mass splittings and the XDM (iDM) mechanism

In contrast to the above values of α_g, the paradigm of ref. [1] would at first seem to suggest smaller values $\alpha_g \sim 10^{-3}$, because the radiative mass splittings of the DM multiplets go like $\alpha_g \mu$ (where μ is the scale of the gauge bosons masses) and it was presumed that $\mu \sim 1$ GeV as the largest value compatible with no production of antiprotons by the decays of the gauge bosons after $\chi\chi \to BB$ annihilation in the galaxy. Since the XDM hypothesis requires χ mass splittings of order MeV, $\alpha = \text{MeV/GeV} \sim 10^{-3}$ would be indicated.

However we have argued above that lighter gauge boson masses $\mu \sim 100$ MeV are in better agreement with gamma ray constraints. The generic estimate $\delta M \cong \frac{1}{2}\alpha_g \mu$ gives ~ 2 MeV for such masses and the preferred coupling $\alpha_g \cong 0.04$ from section V A. This is in just the right range for having excited DM states which can decay to e^+e^- and the ground state.

For other applications, like the iDM mechanism for DAMA, or our inverted mass hierarchy variant of XDM [50], it is desirable to have splittings which are perhaps smaller than the MeV scale. In section VII B 2 we will show that with sufficiently complicated Higgs sectors (three triplets in this example) it is possible to reduce the mass splittings below the generic level of $\alpha\mu$. It is also possible to design the gauge symmetry breaking (by appropriate choices of VEV's or the DM representation) so that no χ mass splittings are induced by gauge boson radiative corrections; for doublet dark matter this is true regardless of the Higgs respresentations. In that case, the splittings must come from Yukawa couplings and then it is possible to decouple the scale of the gauge boson masses from that of the splitting.

It should be emphasized that getting the excited dark matter (XDM) mechanism to produce a large enough signal to explain the INTEGRAL/SPI observations is not as easy as just having the right DM mass splitting; one must generically saturate partial wave unitarity bounds for the excitation cross section to get a large enough rate [68]. We leave the details of reanalyzing this problem to work in progress [69]. The same can be said (even more so) of the iDM mechanism for DAMA. The region of parameter space consistent with the DAMA annual modulation as well as other direct detection experiments is essentially excluded [52], [53]. We give less emphasis to trying to implement the iDM mechanism.

D. Overcoming diffuse gamma ray and CMB constraints

We have already seen that constraints from gamma rays originating as brehmsstrahlung or inverse Compton scattering of the emitted leptons can often rule out models which would have provided good fits to the PAMELA and Fermi observations [32]-[45]. Not only annihilations within our own galaxy provide such constraints, but the accumulated effect from early redshifts and other halos on the CMB and diffuse gamma ray background can be severe. For example, ref. [42] obtains the 95% c.l. CMB bound

$$\langle \sigma v_{\rm rel} \rangle < 4 - 8 \times 10^{-24} \text{cm}^3/\text{s} \tag{36}$$

for the model with $\chi\chi \to 4e$ and $M_\chi = 1-2$ TeV (where their efficiency factor f for transfering energy to the intergalactic medium is approximately 0.9). This is barely compatible with the fit to PAMELA/Fermi/HESS for the same model in ref. [25], reproduced in fig. 7.

Many papers which place gamma ray constraints on annihilating DM assume that only two leptons are produced, instead of the four which are predicted by the class of models we are considering. Given that the preferred models are near the borderline of being excluded, subject to large astrophysical uncertainties, the distinction between the relatively hard, monoenergetic input spectrum for two-lepton annihilations versus the softer four-body final states is important. In particular, ref. [18] (see section 4.1.3) has quantitatively shown this to be the case.

Furthermore, in excluding a given model, one should keep in mind the correlation between the best fit model parameters (the DM mass, annihilation cross section, and gauge boson decay branching ratios) with the assumed DM galactic density profile, since varying the latter can cause significant changes in the former. For example some papers refer to best-fit models as determined by ref. [25], but use different DM profiles to compute the constraints than those used to fit the PAMELA/Fermi data, making it unclear which models are really ruled out.

E. Relic dark gauge (or Higgs) bosons and big bang nucleosythesis

In this section we consider cosmological constraints on the lightest stable or metastable particle in the dark sector. Since we have identified the mass scale $\mu \cong 100$ MeV for the portal boson as being favored by fits to the PAMELA/Fermi/HESS data, we will take this to be the lightest particle, be it the gauge boson in the case of gauge kinetic mixing, or a Higgs boson in the case of Higgs mixing. By this assumption we avoid the introduction of any scales which are even lower than 100 MeV.

Some of the bounds we derive implicitly assume that the dark gauge bosons were in equilibrium with the rest of the plasma at a high temperature, so that their abundance is known around the time when they are becoming nonrelativistic. Even if the mixing parameter ϵ is too small for interactions with electrons to achieve thermal equilibrium with the dark sector, one should remember that kinetic mixing arises from some higher scale physics, such as a heavy X particle which transforms under both the dark and the SM gauge symmetries; recall eq. (9). Even for small values of ϵ, such an origin for the kinetic mixing can insure equilibrium between the dark and SM sectors at the TeV scale.

1. Long-lived gauge bosons

In previous sections, it was noted that dark gauge bosons with long $\sim 10^{12}$ s lifetimes could have provided an escape from gamma ray constraints on annihilating DM through the mechanism of ref. [20], but we now argue these would also dominate the energy density of the universe at the time of BBN, assuming the DM was produced thermally. Let us consider the least dangerous case of $\mu = 10$ MeV gauge bosons. Further, suppose that the SM becomes supersymmetric above the weak scale, so that the number of degrees of freedom is doubled; if instead there is a desert of no new states, this will only make the BBN constraint stronger. When the DM particles freeze out between $T = M_\chi$ and $M_\chi/20$, they transfer their entropy to the dark gauge bosons. This increases the energy density of the latter by at most a factor of two, since there are more gauge degrees of freedom than DM ones. In the meantime, between temperatures of 1 TeV and $\mu = 10$ MeV, the SM degrees of freedom are differentially heated relative to the dark gauge bosons by a factor of approximately $(214/11/2)^{1/3} \cong (9.7)^{1/3}$, due to the change in the number of degrees of freedom from 214 to 11, and the fact that the gauge bosons had been heated by a factor of ~ 2 by the DM annihilations. (The precise value depends on the dimension d_R of the DM representation, but for the small-d_R models we consider, this has no effect on the ensuing bound.) Thus at $T = 10$ MeV, the energy density in dark gauge bosons is suppressed by a factor of $(9.7)^{4/3} \cong 21$ per degree of freedom. By $T = 1$ MeV this suppression has gone down to a factor of 2.1 due to the gauge bosons being nonrelativistic. However there are 3 colors and 3 polarizations, so this counts as approximately 4.5 extra species, and is ruled out. We conclude that the gauge boson lifetime should be less than 1 s (the time corresponding to $T = 1$ MeV), requiring that

$$\epsilon > 4 \times 10^{-11} \left(\frac{100 \text{ MeV}}{\mu}\right)^{1/2} \tag{37}$$

We used the decay rate $\Gamma \cong \frac{1}{3}\alpha\epsilon^2\mu$ for $B \to e^+e^-$.

Even if the thermal relic DM density is highly depleted by having a large annihilation cross section, the above arguments hold, since most of the energy of the original thermal DM population is deposited in the gauge bosons, regardless of how much DM is left. The only obvious way to avoid the above constraint on ϵ is to somehow dilute the original DM even more relative to the SM, *e.g.,* by having even more extra degrees of freedom present at a TeV than in the minimal supersymmetric standard model. We note that the B bosons will not equilibrate with the SM for values of ϵ lower than (37), so equilibration cannot serve to dilute the dark gauge bosons.

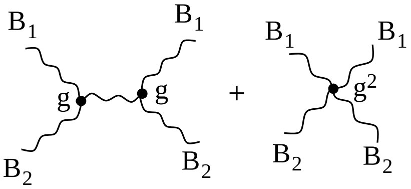

FIG. 8: Annihilations which deplete density of stable B_2 bosons.

2. Stable gauge bosons

Typically only one color of the dark gauge bosons mixes with the SM, say B_1, while transitions between B_2 and B_3 can be mediated by the nonabelian mixing interaction $g\epsilon\cos\theta_W F_{\mu\nu} B_2^\mu B_3^\nu$ which we referred to previously in section II C, leaving the lighter of these two states stable against decay. We must verify that its relic density is not too large.

For definiteness, suppose the stable gauge boson is B_2. The most efficient process for depleting B_2 is the scattering $B_2B_2 \to B_1B_1$, shown in fig. 8, followed by the decays $B_1 \to e^+e^-$. We will show that this is true even if B_1 is heavier than B_2.

The cross section for $B_2B_2 \to B_1B_1$ can be estimated as

$$\langle\sigma v\rangle \sim e^{-\Delta E/T}\, \frac{\alpha_g^2}{\mu^2} \left(\frac{\delta\mu}{\mu}\right)^{1/2} \tag{38}$$

where ΔE is the energy barrier: $\Delta E = 0$ if $\mu_2 > \mu_1$, and $\Delta E = 2\delta\mu = 2(\mu_2 - \mu_1)$ if $\mu_1 > \mu_2$. The factor of $(\delta\mu/\mu)^{1/2}$ arises from the velocity of the final state particles, which is 1 in the more familiar case of annihilation to light final states. The freeze-out temperature for this reaction is determined as usual by setting $n_{B_2}\langle\sigma v\rangle$ equal to the Hubble rate, using the equilibrium density of a massive particle for n_{B_2}; one finds that

$$\begin{aligned} x_f = \frac{\mu}{T_f} &= \frac{\ln\left(0.04\frac{\alpha_g^2}{\sqrt{g_*}}\frac{m_P}{\mu}\right) - 2\ln x_f}{1 + \Delta E/\mu} \\ &\cong \frac{35.4 - 2\ln x_f}{1 + \Delta E/\mu} \end{aligned} \tag{39}$$

for $\mu = 100$ MeV and $\alpha_g = 0.04$. This implicit equation quickly converges to a solution by iteration. Values of x_f as a function of $\Delta E/\mu$ are shown in figure 9.

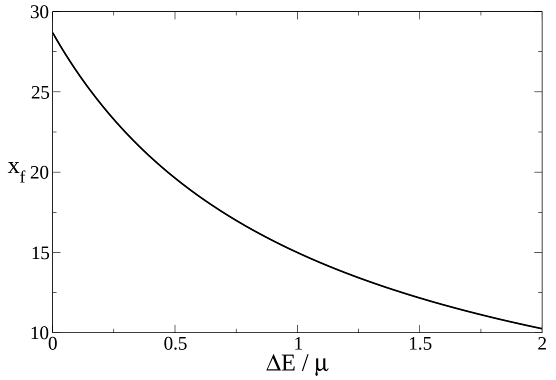

FIG. 9: Freeze-out value x_f versus $\Delta E/\mu$ (solution of eq. (39)) for the process $B_2B_2 \to B_1B_1$, where $\Delta E = \max(2(\mu_1 - \mu_2), 0)$.

As long as the interactions of fig. 8 are in equilibrium, the abundance Y_{B_2} tracks that of Y_{B_1}, whose principal connection with the SM is through the decays and inverse decays $B_1 \leftrightarrow e^+e^-$. The decay rate is suppressed by ϵ^2, and for the small values of ϵ we obtain in the ensuing bound, it is consistent to neglect scattering processes $B_1B_1 \leftrightarrow e^+e^-$ whose rate goes like ϵ^4. In appendix D we show that the processes $BBB \to BB$ are able to keep the gauge bosons in kinetic equilibrium with themselves down to a temperature given by $x_k = \mu/T_k = 17.5$, so B_1 would maintain the equilibrium abundance of a nonrelativistic particle $Y_{\rm eq}$ until this temperature. At lower temperatures, it disappears due to its decays:

$$Y_{B_1} = Y_{\rm eq}(x_k)e^{-\Gamma t} = Y_{\rm eq}(x_k)e^{-(\Gamma/H(\mu))x^2} \tag{40}$$

where $\Gamma = \frac{1}{3}\alpha\epsilon^2\mu$ is the decay rate, $x = \mu/T$, and $H(\mu)$ is the Hubble rate at $T = \mu$. Since $Y_{\rm eq}(x) \sim x^{3/2}e^{-x}$, we find that $Y_{\rm eq}(x_k) \cong 2 \times 10^{-6}$. The analysis of ref. [70] shows that a good estimate of the relic abundance of B_2 is obtained by evaluating Y_{B_1} (which is the source for Y_{B_2} in the Boltzmann equation) at x_f: $Y_{B_2}(\infty) = Y_{B_1}(x_f)$. On the other hand, the present abundance of stable B_2 bosons must not exceed the observed DM abundance. Using baryons as a reference,

$$Y_{B_2}(\infty) < \frac{\Omega_{DM}}{\Omega_b}\frac{m_N}{\mu}\eta_b \cong 3 \times 10^{-8} \tag{41}$$

where $\Omega_{DM}/\Omega_b \cong 5$, $\eta_b \cong 6 \times 10^{-10}$, m_N is the mass of the nucleon, and we took $\mu = 100$ MeV. Putting these results together, we obtain the bound

$$\begin{aligned} \epsilon &> \frac{1}{x_f}\left(\frac{3(\ln(\frac{1}{3}\times 10^8) - x_k + \frac{3}{2}\ln x_k))}{1.67\sqrt{g_*}\alpha}\,\frac{\mu}{M_p}\right)^{1/2} \\ &= \frac{9 \times 10^{-9}}{x_f} \end{aligned} \tag{42}$$

Since $x_f < 28.7$ (the value when $\Delta E = 0$), this is approximately an order of magnitude stronger than the bound (37) from nucleosynthesis.[4]

3. *Long-lived Higgs bosons*

We now consider the case where the Higgs boson S that mixes with the SM is the lightest metastable state of the dark sector. The gauge bosons provide no more constraint in this case since they are presumed to be heavier, and although they are stable, they efficiently annihilate into dark sector Higgses with a negligible relic density, $\sim (\mu/M_\chi)^2$ smaller than the closure density.

If the coupling of the Higgs to the SM is too strongly suppressed by the small mixing angle θ, there will be similar problem as the one involving metastable gauge bosons, discussed above. The Higgs should decay before nucleosynthesis to avoid dominating the energy density of the universe. We can directly adapt the result (37) by replacing $\epsilon \to \theta$, $\mu \to m_S$, $e \to y_e$ (the electron Yukawa coupling, $y_e = y_t m_e/m_t \cong 3 \times 10^{-6}$):

$$\theta > 4 \times 10^{-6}\left(\frac{100 \text{ MeV}}{m_S}\right)^{1/2} \tag{43}$$

Of course, this also forbids the possibility of a long-lived intermediate state [20] for transporting them outside the galactic center before decaying into e^+e^-.

F. Long-lived intermediate DM states and direct detection constraint

In section IV we discussed the implications of an absolutely stable intermediate DM state, protected by a discrete symmetry. This symmetry also made the models safe from downward transitions $\chi_2 \to \chi_1$ mediated by nuclear recoil in direct detection experiments, since the gauge boson B_3 was forbidden from mixing with the SM. However, if the symmetry is not present and B_3 does mix with hypercharge, interesting constraints can arise, since the state χ_2 generically has a lifetime longer than the age of the universe, has a significant relic density, and can undergo $\chi_2 \to \chi_1$ in the detector [53]. The latter process is not kinematically suppressed since it is exothermic, and it leads to strong constraints on the mixing parameter ϵ. Ref. [53] finds the 90% c.l. limit $\epsilon < 2 \times 10^{-6}$ from CDMS for $M_\chi = 1$ TeV, $\delta M_{12} = 100$ keV for the small splitting which would be relevant for the iDM explanation of DAMA, and $\mu = 1$ GeV. As explained above, we

---

[4] If $x_f < x_k$, then the bound is slightly modified since B_1 maintains equilibrium density until x_f:

$$\epsilon > \frac{4 \times 10^{-9}}{x_f}\left(17.3 + \tfrac{3}{2}\ln x_f - x_f\right)^{1/2}$$

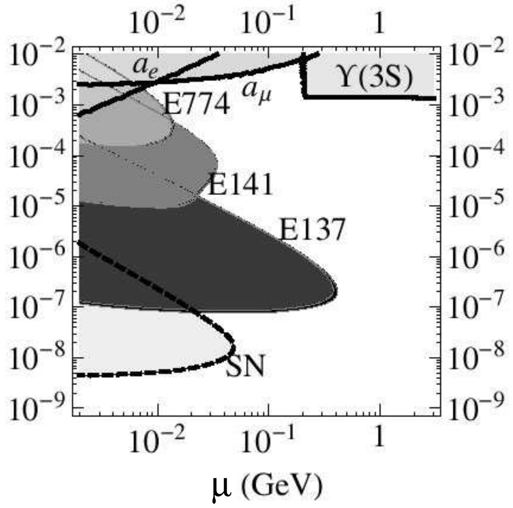

FIG. 10: Experimental constraints on ϵ versus gauge boson mass μ taken from ref. [71]. Enclosed regions are excluded by anomalous magnetic moments, beam dump experiments and supernovae.

prefer $\mu = 100$ MeV, which makes the constraint even more severe,

$$\epsilon < 2 \times 10^{-8} \left(\frac{\mu}{100 \text{ MeV}} \right)^2 \tag{44}$$

since the χ-nucleon cross section scales like ϵ^2/μ^4.

Notice that the window between (44) and our BBN or relic density bounds (37,42) is only a few orders of magnitude. This region of parameter space is also below those which could be probed by complementary experiments, as illustrated in fig. 10, taken from ref. [71] (see also ref. [72],[73].) In the models we consider, the bound (44) can be evaded if we insist upon the Z_2 symmetry which forbids the transitions leading to direct detection. This makes it possible to have models which could also be probed by laboratory experiments such as beam dumps. Another way to evade (44) can arise if the mass splitting between the intermediate and ground state is *too large* [73], since direct detection experiments do not look for very large recoil energies. The inverted mass hierarchy could thus be useful for this purpose even if there is no Z_2 symmetry and the intermediate state is only metastable.

VI. DOUBLET DARK MATTER

We now begin our investigation of more specific classes of models, organized according to the SU(2) representation under which the DM transforms. If the DM is in the doublet representation, it must be vector-like (Dirac) in order to have a bare mass term,

$$M \bar{\chi}^i \chi_i \tag{45}$$

In this case, DM number becomes conserved. Its abundance could be due to its chemical potential rather than freeze-out, similar to the baryon asymmetry, and so a nonthermal origin could be considered more natural than for Majorana DM.

There is no way to split the masses of the doublet through radiative corrections from the gauge bosons, because each member of the doublet has equal-strength interactions with all three gauge bosons. For example suppose only B_1 were to get a mass μ_1; the contribution to the χ mass matrix is $\delta M_{ik} = -\frac{1}{2}\alpha\mu_1\tau^1_{ij}\tau^1_{jk} = -\frac{1}{2}\alpha\mu_1\delta_{ik}$. But we can get a splitting through the VEV of a triplet via the Yukawa interaction

$$h \chi^\dagger \tau^a \chi \Delta^a_3 \tag{46}$$

The suffix on Δ_3 is a mnemonic for the fact that (for convenience) we take its VEV to be in the $a = 3$ direction, since this gives the mass splitting $\pm h\Delta_3$ between the Dirac states χ_1 and χ_2.

A. Gauge kinetic mixing

Let us first consider the case of gauge kinetic mixing as the portal to the SM. With the above mass splitting, either B_1 or B_2 must mix with the SM hypercharge so that transitions between χ_2 and χ_1 can occur, with the production of e^+e^-. The triplet VEV which generates the mass splitting is not suitable for generating the kinetic mixing of the gauge boson via $\frac{1}{\Lambda}Y_{\mu\nu}B^{\mu\nu}_a\Delta^a_3$. In fact, such mixing is dangerous from the standpoint of constraints from direct DM searches, since it would induce diagonal couplings via B_3 of the DM to nuclei. One possibility is to have an additional triplet, Δ^a_1, coupling as in eq. (1), which gets a VEV along the 1 (or 2) direction. The extra triplet VEV serves another purpose, by completely breaking the SU(2) gauge symmetry, whereas a single triplet would break SU(2)→U(1). Assuming that Δ_1 gets its VEV along the 1 direction, the spectrum of the gauge bosons is

$$\mu_1 = g\Delta_3, \quad \mu_2 = g\sqrt{\Delta_3^2 + \Delta_1^2}, \quad \mu_3 = g\Delta_1 \tag{47}$$

With this spectrum and the couplings described above, B_3 is stable, but B_2 can decay into $B_3\,\gamma$ via the non-abelian gauge mixing interaction $\epsilon g c_W F_{\mu\nu} B^\mu_2 B^\nu_3$. If we assume that $\Delta_1 > \Delta_3$, then annihilations $B_3B_3 \to B_1B_1$ effectively deplete any potentially dangerous B_3 relic density in the early universe.

Alternatively, kinetic mixing could be accomplished by a Higgs doublet as in eq. (2), with VEV $h = (v/\sqrt{2})(1,1)^T$. This would cause mixing of only B_1 to the SM. The gauge boson mass spectrum in this case is

$$\mu_1 = \mu_2 = g\sqrt{\Delta_3^2 + v^2} \quad \mu_3 = gv. \tag{48}$$

Similarly to the case of two triplets, B_2 can decay into $B_3\,\gamma$, but for this spectrum, the $B_3B_3 \to B_1B_1$ annihilation channel is kinematically blocked. Therefore the

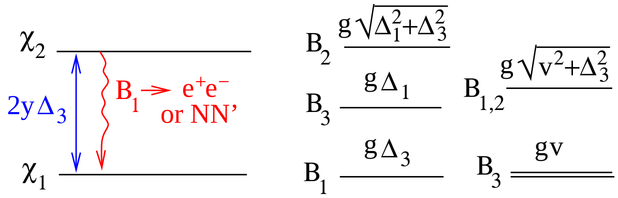

FIG. 11: Spectrum of doublet χ states (left) and two possibilities for gauge boson spectra discussed in the text (center and right).

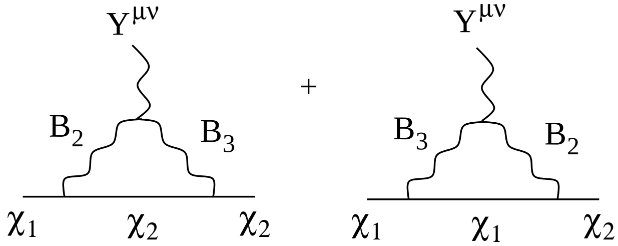

FIG. 12: Canceling loop diagrams contributing to the transition magnetic moment of doublet DM.

mixing parameter ϵ must satisfy (42) to effectively deplete the relic B_3's. The mass levels for the DM and gauge boson states are summarized in figure 11.

As mentioned in the previous section, doublet DM has the advantage of allowing the gauge coupling to be as large as needed for getting the right annihilation cross section, without additional constraints from the size of the χ_1-χ_2 mass splitting, $\delta M = 2h\Delta_3$. For example one can adopt close to the preferred value from section V, $\alpha_g = 0.054$ (notice that this gives the correct relic density for doublet DM, eq. (36), if $M_\chi = 700$ GeV, compatible with the allowed region in fig. 7), and take the gauge boson mass at the 100 MeV scale, assuming the argument of the previous section that diffuse gamma ray constraints prefer the $4e$ annihilation channel over an admixture of e and μ. The triplet VEV's are then of order $\mu/g \sim \mu \sim$ 100 MeV, and the Yukawa coupling should be $h \sim 10^{-2}$ to accommodate the excited DM (XDM) mechanism for explaining INTEGRAL/SPI.

A distinctive feature of the doublet DM model is that its transition magnetic moment is suppressed relative to that of triplet DM. The diagrams which contribute are shown in figure 12. The group theory factors from the DM gauge couplings of the two diagrams are respectively $\tau_{22}^2\tau_{21}^2$ and $\tau_{21}^2\tau_{11}^2$ (the Pauli matrices), which are equal and opposite. Therefore the sum of the diagrams is suppressed by the small mass difference $\delta M/M$ and the gamma ray line from $\chi_2 \to \chi_1\gamma$ decays is too weak to be detected by INTEGRAL. The constraint $\alpha_g < 0.08$, eq. (18), does not apply.

B. Higgs mixing

Since we have argued that a DM Yukawa coupling (46) to a triplet is already necessary to get the doublet mass splitting, it is tempting to make a more economical model without gauge kinetic mixing, by letting this triplet mix with the SM Higgs through a $\lambda|H|^2|\Delta_3|^2$ coupling. The most stringent of the constraints on λ from section III B is (23), arising from direct detection of the DM. For $h = 10^{-2}$ this gives $\lambda < 3\times 10^{-2}$ if $m_{\Delta_3} \cong 200$ MeV and $\langle\Delta_3\rangle \cong 1$ GeV. Saturating this inequality leads to the mixing angle $\theta \cong 2\times 10^{-4}$, according to (22). This value is consistent with our BBN constraint (43).

C. Diagonal couplings to B_3

Even though we took care to avoid the direct annihilation channel $\chi_1\chi_1 \to e^+e^-$ through virtual B_3 production, by forbidding mixing between B_3 and the SM hypercharge, it is impossible to forbid $\chi_1\chi_1 \to B_1 B_2$. If only B_1 couples to the SM but not B_2, this results in the final state $e^+e^-B_2$, where B_2 is invisible. In the foregoing we have noted that the two-body final state e^+e^- is ruled out, because its spectrum has the wrong shape to fit the PAMELA and Fermi observations. The three-body final state is much more similar to the four-body one in this respect, however, because the two visible leptons share the energy of the incoming χ's with the B_2. They thus have a soft spectrum which is qualitatively similar to that of the four-body case. Thus the $\chi\chi \to e^+e^-B_2$ channel in this model is on a similar footing to the $\chi\chi \to 4e$ one in models with Majorana DM. If B_2 also mixes with the SM hypercharge so that $B_2 \to e^+e^-$, they become identical.

VII. TRIPLET DARK MATTER

We now take χ_a to be a real (Majorana) triplet of SU(2). It can have a bare Majorana mass $M\chi^a\chi^a$. In this case, mass splittings can be generated radiatively, as well as at tree level. A doublet VEV h gives equal contributions to all the gauge boson masses, so it does not generate any mass splittings between the χ_a's. It is thus more economical to assume there is at least one triplet VEV contributing to the SU(2) breaking. However this is not enough to fully split the DM states, since a single triplet VEV would leave two of the gauge bosons degenerate in mass, and the radiative corrections would then do likewise for the DM states. We are led to introduce either a second Higgs triplet as in the doublet DM case, or a quintuplet. It is also interesting to consider a model with three triplet VEVs, since this gives additional freedom in arranging the DM spectrum to have an inverted or normal hierarchy.[5] In the following, we consider these different Higgs sectors and the χ^a mass splittings that arise due to radiative corrections.

A. Two triplet Higgs fields

Let us turn on VEV's for two triplets in orthogonal directions, Δ_1^1 and Δ_2^2, for example. It is easy to write a Higgs potential whose minima have this property:

$$V = \sum_i \lambda_i(\Delta_i^2 - v_i^2)^2 + \lambda_{12}(\vec{\Delta}_1 \cdot \vec{\Delta}_2)^2 \qquad (49)$$

As long as $\lambda_{12} > 0$, the energy is minimized for orthogonal VEVs.

1. Mass spectra

The gauge boson mass spectrum is

$$\mu_1 = g\Delta_2, \quad \mu_2 = g\Delta_1, \quad \mu_3 = g\sqrt{\Delta_1^2 + \Delta_2^2} \qquad (50)$$

(With no loss of generality, one can take $\Delta_1^1, \Delta_2^2 > 0$ by doing a global gauge transformation.) The radiative corrections to the DM masses are

$$\begin{aligned} \delta M_1 &= -\frac{1}{2}g\alpha\left(\Delta_1 + \sqrt{\Delta_1^2+\Delta_2^2}\right) \\ \delta M_2 &= -\frac{1}{2}g\alpha\left(\Delta_2 + \sqrt{\Delta_1^2+\Delta_2^2}\right) \\ \delta M_3 &= -\frac{1}{2}g\alpha(\Delta_1 + \Delta_2) \end{aligned} \qquad (51)$$

Depending on the ratio Δ_2/Δ_1, this can correspond to either the normal or inverted hierarchy. To see the range of possibilities, define $\Delta_1 = \Delta\cos\theta$ and $\Delta_2 = \Delta\sin\theta$, and subtract from each δM_i the average splitting (since this just renormalizes the bare value M_χ):

$$\begin{aligned} \delta M_1 &\to -\frac{1}{6}g\alpha\Delta\,(1+\cos\theta - 2\sin\theta) \\ \delta M_2 &\to -\frac{1}{6}g\alpha\Delta\,(1+\sin\theta - 2\cos\theta) \\ \delta M_3 &\to -\frac{1}{6}g\alpha\Delta\,(-2+\cos\theta + \sin\theta) \end{aligned} \qquad (52)$$

The spectrum is plotted as a function of θ (which lies in the range $[0,\pi/2]$ due to our requirement that both VEVs be positive) in figure 13. There it is clear that the inverted hierarchy occurs if $\theta \ll 1$ ($\Delta_2 \ll \Delta_1$) or $\theta \cong \pi/2$ ($\Delta_1 \ll \Delta_2$), while the normal one occurs if $\theta \cong \pi/4$ ($\Delta_1 \cong \Delta_2$).

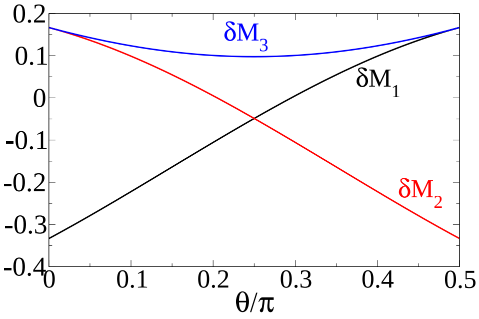

FIG. 13: Mass splittings of triplet χ states for the model with two orthogonal triplet VEVs as a function of $\theta = \tan^{-1}(\Delta_2/\Delta_1)$, eq. (52), in units of $\alpha g\sqrt{\Delta_1^2+\Delta_2^2}$.

2. Inverted hierarchy and Z_2 symmetry

To discuss the phenomenology of this model, we must specify which of the gauge kinetic mixing operators $\vec{\Delta}_i \cdot \vec{B}_{\mu\nu}F^{\mu\nu}/\Lambda_i$ are assumed to be turned on. The simplest possibility, and the one that allows for Z_2 symmetry, is that only one of them is significant, say the one corresponding to $\vec{\Delta}_1$. Then only B_1 mixes with the SM, and we can assign Z_2 charges to B_2, B_3, χ_2, χ_3. The uncharged state χ_1 cannot decay into χ_2, so to implement the inverted hierarchy for INTEGRAL, we should choose $\theta \lesssim \pi/2$ to make χ_1 the intermediate state.

By choosing $\theta \cong \pi/2$, hence $\Delta_1 \ll \Delta_2$, we obtain from (50) the gauge boson mass spectrum $\mu_2 < \mu_1 \lesssim \mu_3$. According to the argument of section V E 2, the gauge mixing parameter must then exceed the lower bound (42).

To be compatible with a nonthermal origin, the gauge coupling must be larger than $\alpha_g = 0.03$, according to eq. (36). Taking $\alpha_g = 0.06$ and $\mu \cong g\Delta = 100$ MeV, for example, the gauge coupling is then $g = \sqrt{4\pi\alpha_g} = 0.87$, and $\Delta = \mu/g = 115$ MeV. The largest mass splitting is of order $\frac{1}{2}\alpha\mu = 3$ MeV. We have the freedom to adjust the smaller splitting as desired by choosing $\theta = \tan^{-1}(\Delta_2/\Delta_1)$. Taking $\theta = 0.4\pi$ gives $\delta M_{23} = 2.1$ MeV and $\delta M_{13} = 150$ keV, which is small enough to comfortably enhance the 511 keV signal to the level observed by INTEGRAL [69].

3. Normal hierarchy

Since it might be argued that the window for iDM to explain the DAMA/LIBRA annual modulation is not completely closed [74], for completeness we consider the case of the normal mass hierarchy. As is clear from fig. 13, it arises from choosing θ close to $\pi/4$. If one wants to have both the iDM and XDM effects for DAMA and INTEGRAL, respectively, then B_3 must mix with the SM hypercharge, in addition to B_1 (if $\theta > \pi/4$) or B_2 (if $\theta < \pi/4$). Interestingly, the spectrum (48) shows that the boson which does not mix with the SM is the lightest one, while B_3 is the heaviest. Therefore the lightest gauge boson is stable and the BBN bound (42) on ϵ applies to this model.

---

[5] We prefer the inverted hierarchy since it can boost the effectiveness of XDM, and avoid the direct detection constraint (44).

With the normal hierarchy there is no requirement for a nonthermal origin of the DM, so we consider the value $\alpha_g = 0.03$, eq. (36), needed for the correct thermal relic density, and the boost factor 300 needed for PAMELA/Fermi. The gauge coupling is $g = 0.61$. Fig. 1 of ref. [1] shows that this value of the coupling gives approximately the required value of the boost factor for $\mu \lesssim 1$ GeV, assuming the DM velocity dispersion of $\sigma = 150$ km/s. We are free to adjust the triplet VEVs to obtain the desired mass splittings. For example with $\delta M_{13} \sim \delta M_{23} \cong 2$ MeV, one finds $\Delta_1 \sim \Delta_2 \cong 750$ MeV. To get a small mass splitting $\delta M_{12} = \frac{1}{2} g\alpha_g(\Delta_1 - \Delta_2)$ of order 100 keV, if one wishes to explain DAMA, the two VEV's Δ_1 and Δ_2 have to be tuned to be equal to each other to within one part in 70.

4. Nonorthogonal VEVs

For a generic Higgs potential, Δ_1 and Δ_2 are not orthogonal (*e.g.*, Δ_2 could be nonzero in both the 1 and 2 directions.). Aside from changing the details of the gauge masses and fermion mass splittings, this has the same effect as turning on kinetic mixing terms for both B_1 and B_2. This is because the mass eigenstates of the vectors become mixtures of these two directions; the gauge interactions of the mass eigenstates with the χ_a can be put in canonical form with a corresponding rotation of $\chi_{1,2}$. In this basis, the χ_a are mass eigenstates. However, the B vector that mixes with the SM hypercharge vector is a linear combination of both the B_1 and B_2 mass eigenstates, so both the $\chi_2 \leftrightarrow \chi_3$ and $\chi_1 \leftrightarrow \chi_3$ transitions couple to the SM. This implies there is no Z_2 symmetry protecting the intermediate state, in the inverted hierarchy case. Thus it is important to keep the VEVs orthogonal in that case, whereas relaxing this assumption does not hurt the normal hierarchy scenario. In fact it makes it simpler, by requiring only a single gauge kinetic mixing term to be nonnegligible, while still coupling both DM transitions to the SM, as required by the iDM and XDM mechanisms.

B. Three triplet Higgs fields

1. Generic VEVs

For a generic Higgs potential with three triplet Higgs fields, we can use gauge transformations to align $\vec{\Delta}_1$ in the 1 direction, with $\Delta_1^1 > 0$, and $\vec{\Delta}_2$ in the 1-2 plane with $\Delta_2^2 > 0$, while the direction of $\vec{\Delta}_3$ remains general. The vacuum manifold can thus be parametrized by an overall amplitude $\Delta = (\sum_i |\vec{\Delta}_i|^2)^{1/2}$ and five angles: two measuring the relative amplitudes of the three VEVs (covering 1/8 of a sphere), one determining the orientation of $\vec{\Delta}_2$ (covering 1/2 of a circle), and two controlling the orientation of $\vec{\Delta}_3$ (on a full sphere). Depending on the vacuum state, the DM mass splittings can take on any hierarchy. Unlike the previous case, χ_3 need not be the heaviest DM state.

At a generic position in the vacuum space, all the B mass eigenstates mix with the SM hypercharge vector. Assuming $m_1 \lesssim m_2 \ll m_3$ in a normal hierarchy, one can implement both the iDM and XDM dark matter excitation mechanisms. There are transition magnetic moments between all pairs of χ_i and χ_j allowing for single-photon decays of χ_2 and χ_3. The exception is for $\Delta_2^1 = \Delta_3^1 = 0$; in that case, there is an unbroken Z_2 symmetry, and only B_1 mixes with the SM. Then either iDM or XDM is possible (not both), and one of the excited DM states will be stable.

2. Orthogonal VEVs

The potential (49) can be generalized to one that leads to three orthogonal triplet VEVs:

$$V = \sum_i \lambda_i(\Delta_i^2 - v_i^2)^2 + \Big[\eta_1(\vec{\Delta}_2 \cdot \vec{\Delta}_3)^2 + \text{cyc. perm.}\Big] \tag{53}$$

As long as the η_i couplings are positive, the desired vacuum state is a minimum of the potential. There is no obstacle to assuming that only B_1 mixes with the SM vectors, if one wants to incorporate the Z_2 symmetry that prevents χ_1 from decaying. We will show that both normal and inverted DM mass hierarchies are possible, with χ_1 as the intermediate state. Many configurations of the VEVs are compatible with the iDM and/or XDM mechanisms.

Taking each of the respective fields $\vec{\Delta}_i$ to align along the ith direction, the gauge boson masses are given by $\mu_1 = g\sqrt{\Delta_2^2 + \Delta_3^2}$ and cyclic permutations, while the χ mass splittings are $\delta M_1 = -\frac{1}{2}\alpha_g\,(\mu_2 + \mu_3)$ plus cyclic permutations. The full range of possibilities for the spectrum can be explored by parametrizing the VEVs in spherical coordinates,

$$\begin{aligned}\Delta_1 &= \Delta\sin(\theta)\cos(\phi)\\ \Delta_2 &= \Delta\sin(\theta)\sin(\phi)\\ \Delta_3 &= \Delta\cos(\theta)\end{aligned} \tag{54}$$

where $\Delta = (\sum_i \Delta_i^2)^{1/2}$, and the angles are restricted by $0 \le \theta \le \pi/2$ and $0 \le \phi \le \pi/2$ so that each Δ_i is positive. The resulting δM_i's, shifted to set the average value $\frac{1}{3}\sum_i \delta M_i$ to zero, are shown in figure 14.

To obtain the inverted hierarchy, where χ_1 is the intermediate state with a mass close to the heaviest state, one possibility is to take $\Delta_3 \ll \Delta_1, \Delta_2$, which essentially reproduces the two Higgs case studied above. This corresponds to $\theta \cong \pi/2$ and $\phi \lesssim \pi/2$ in fig. 14, with χ_2 and χ_3 being respectively the ground state and highest excited

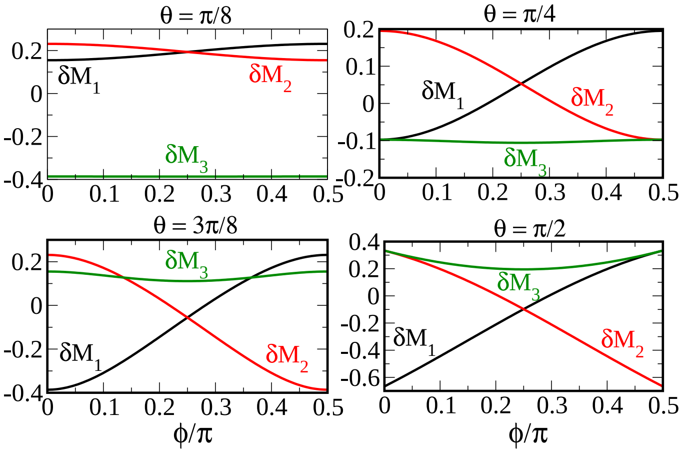

FIG. 14: Spectrum of triplet χ states for model with three triplet VEVs parametrized as in (54) and with the average mass shift subtracted. δM_i are in units of $g\alpha_g\Delta/2$. Each panel shows a different value of θ.

state. The other possibility is to take $\Delta_3 \gg \Delta_1 \gtrsim \Delta_2$, corresponding to $\theta \cong 0$ and $\phi < \pi/4$, in which case χ_3 is the lowest mass state. From fig. 14 one can also see examples of the normal hierarchy, for example near $\theta = \pi/2$ and $\phi = \pi/4$.

It is interesting to notice that smaller mass splittings than the generic scale $\alpha_g\mu$ can be obtained near special values of the VEVs. When Δ_1 and Δ_2 are equal, $\phi = \pi/4$, the masses M_1 and M_2 become accidentally degnerate. By tuning the VEVs to be close to this point, the 100 keV scale desired for the iDM splitting can be achieved even if $\alpha_g\mu$ has the right magnitude for getting the XDM splitting.

C. Quintuplet Higgs field

Allowing DM to couple to a quintuplet Higgs field, which is a symmetric traceless tensor Σ_{ab}, gives further flexibility in model building, since the pattern of gauge boson masses induced by the Σ VEV is different than for triplets, and one also has the possibility of a Yukawa coupling $y\chi_a\Sigma_{ab}\chi_b$ to give tree-level contributions to the DM mass splitting. In addition one still wants at least one triplet or doublet Higgs to generate kinetic mixing of one of the B's to the photon.

For a fairly general class of potentials, the VEV of Σ can be chosen to be along the diagonal components. Let us take this as a simplifying assumption and show how much can be accomplished with just the two components, which we denote by

$$\langle\Sigma\rangle = \frac{1}{\sqrt{2}}\begin{pmatrix} A-B & & \\ & 2B & \\ & & -A-B \end{pmatrix} \tag{55}$$

(note the different normalization of B than for the corresponding quintuplet χ field in (32)). If $\langle\Sigma\rangle$ is much larger than the triplet or doublet VEV, the resulting spectrum of gauge boson masses is approximately

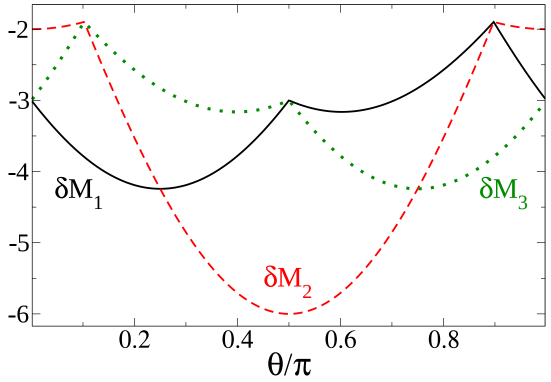

FIG. 15: Mass splittings of triplet χ states for model with two components of quintuplet VEV, eq. (55), parametrized by $\tan\theta = B/A$. δM_i are in units of $\frac{1}{2}g\alpha_g\sqrt{A^2+B^2}$.

$$\mu_1 = g\,|A+3B|\,,\quad \mu_2 = g\,|2A|,\quad \mu_3 = g\,|A-3B| \tag{56}$$

where we used the generators

$$T^d_{ab,ce} \sim i(\epsilon_{adc}\delta_{be} + \epsilon_{bde}\delta_{ac}) \tag{57}$$

where "∼" denotes that the expression must be symmetrized on *ab* and *ce*. The radiative mass corrections of the DM states are

$$\begin{aligned} \delta M_3 &= -\frac{1}{2}g\alpha_g\,(|A+3B|+|2A|) \\ \delta M_2 &= -\frac{1}{2}g\alpha_g\,(|A+3B|+|A-3B|) \\ \delta M_1 &= -\frac{1}{2}g\alpha_g\,(|A-3B|+|2A|) \end{aligned} \tag{58}$$

Parametrizing the VEVs by $\tan\theta = B/A$, we obtain the full range of possibilities by letting θ range from 0 to π. Although the region $\pi/2 < \theta < \pi$ can be mapped onto $0 < \theta < \pi/2$ by gauge transformations, the freedom to do so is generally inhibited by VEVs of other Higgs fields such as triplets, which we mention below. The result is shown in fig. 15.

1. *Normal hierarchy*

Fig. 15 shows that the normal hierarchy occurs in the region of $\theta \cong 0$ and $\theta \cong \pi/4$ (with the same shape of spectra at $\theta \cong \pi$ and $\theta \cong 3\pi/4$). For illustration consider the case of $\theta \cong 0$, which corresponds to $B \ll A$. The gauge bosons have the spectrum $\mu_3 \lesssim \mu_1 < \mu_2$. The order of the DM masses is $M_1 \lesssim M_3 < M_2$, and we can turn on transitions between χ_1-χ_2 and χ_1-χ_3 which couple to the electron vector current, by mixing B_3 and B_2 with SM hypercharge. This can be accomplished using two triplets, which we will call $\vec{\Delta}_2$ and $\vec{\Delta}_3$, with VEV's Δ_2^2 and Δ_3^3. A model-building challenge is to find a scalar potential which gives rise to this symmetry breaking pattern together with that assumed for the quintuplet.

We noted above that it is easy to make a potential for triplets that gives rise to orthogonal VEV's. Suppose we do this; then global SU(2) transformations can be used to orient them in the 2 and 3 directions, respectively. Next consider the Σ sector. The term $\lambda(\mathrm{tr}\Sigma^2 - v^2)^2$ is O(5) symmetric under rotations of the vector $(A, B/\sqrt{3}, C, D, F)$, where C, D, F are the off-diagonal components of Σ. To break this symmetry in such a way as to prefer the A, B components, we can add terms

$$\Lambda_2 \Delta_2^T \Sigma \Delta_2 + \Lambda_3 \Delta_3^T \Sigma \Delta_3 \tag{59}$$

which are linear in A and B when the Δ_i get their expected VEVs, and thus lead to nonzero VEVs for A and B. This would be spoiled by a term of the form $\Delta_2^T \Sigma \Delta_3$, but the latter can be forbidden by separate discrete symmetries under which Δ_2 or Δ_3 change sign. These symmetries are weakly broken by the gauge kinetic mixing terms, which would presumably give rise to a small $\Delta_2^T \Sigma \Delta_3$ interaction through loops. This would generate perturbations to the previous analysis due to the presence of small off-diagonal VEVs in Σ_{ab}.

2. *Inverted hierarchy*

Fig. 15 also reveals the inverted hierarchy at $\theta \cong 0.1\pi$, 0.9π and $\pi/2 \pm \epsilon$. The latter occurs when $|A| \ll |B|$. Consider the case $\pi/2 - \epsilon$ where $M_2 < M_1 \lesssim M_3$. We need B_1 to mix with the SM in this case, suggesting a triplet $\vec{\Delta}_1$ with VEV in the component Δ_1^1. One can use an analogous potential to (59), $\Lambda_1 \Delta_1^T \Sigma \Delta_1 + \Lambda_2 \Delta_2^T \Sigma \Delta_2$, to generate VEVs in the A, B components, if we add the additional triplet $\vec{\Delta}_2$, which however does not play any role in the gauge kinetic mixing.

For this scenario, the gauge bosons have the spectrum $\mu_2 < \mu_3 < \mu_1$. Thus B_1 which mixes with the SM is the heaviest. The relic gauge boson constraint (42) then applies, making this model susceptible to laboratory searches for light gauge bosons that mix with the SM.

VIII. QUINTUPLET DARK MATTER

As the highest DM representation we will consider here, we turn to the quintuplet case, where χ_{ab} is a traceless symmetric tensor. The gauge generators in this representation are given in (57), which for conciseness is not symmetrized in its indices, but the actual generator must be symmetrized in ab and ce, with accompanying factor of 1/4. We will label the canonically normalized states of χ_{ab} by

$$\langle\chi\rangle = \begin{pmatrix} A - B/\sqrt{3} & C & D \\ C & 2B/\sqrt{3} & F \\ D & F & -A - B/\sqrt{3} \end{pmatrix} \tag{60}$$

(Notice the change in normalization of B compared to our choice for quintuplet Higgs fields in (55).) These are the mass eigenstates at tree level.

A. Radiative mass corrections

In previous sections we have given explicit expressions for the gauge boson masses assuming various patterns of symmetry breaking. Here we will leave them unspecified and study the χ radiative mass splittings as a function of general values of μ_i. The χ mass splitting term is given by

$$\delta V_{\rm mass} = -\frac{1}{2}\alpha \sum_d \, \mu_d \, \chi_{ab} \, T^d_{ab,ce} T^d_{ce,fg} \, \chi_{fg} \tag{61}$$

For general values of the gauge boson masses, we find

$$\begin{aligned} \delta V_{\rm mass} = \; & -\alpha\mu_1((A+\sqrt{3}B)^2 + C^2 + D^2 + 4F^2) \\ & -\alpha\mu_2(4A^2 + C^2 + 4D^2 + F^2) \\ & -\alpha\mu_3((A-\sqrt{3}B)^2 + 4C^2 + D^2 + F^2) \end{aligned} \tag{62}$$

In the simpler case where $\mu_1 = \mu_3$, the terms which mix A and B cancel and the mass terms are diagonal. The average mass splitting in this case is $-4\mu_1 - 2\mu_2$. Subtracting away this central value, we obtain the hierarchy of mass splittings

$$(A, D) : +2\delta, \quad (C, F) : -\delta, \quad B : -2\delta \tag{63}$$

where $\delta = 4\alpha_g(\mu_1 - \mu_2)$. In the more general case where $\mu_1 = \mu + \delta_1/4\alpha_g$, $\mu_2 = \mu$, $\mu_3 = \mu + \delta_3/4\alpha_g$, we get splittings equal to

$$\begin{aligned} & (A', B') : \pm 2\sqrt{\delta_1^2 - \delta_1\delta_3 + \delta_3^2} \\ & C : \delta_1 - 2\delta_3, \quad D : \delta_1 + \delta_3, \quad F : \delta_3 - 2\delta_1 \end{aligned} \tag{64}$$

These can be parametrized using

$$\delta_1 = \delta\cos\theta, \quad \delta_3 = \delta\sin\theta \tag{65}$$

so that $\delta^2 \equiv 8\alpha_g^2[(\mu_1 - \mu_2)^2 + (\mu_3 - \mu_2)^2]$ controls the overall magnitude of the splittings, whereas θ controls the relative values (and can be in the range $[0, 2\pi]$ since there is no restriction on the signs of the gauge boson mass differences). We get

$$\begin{aligned} \delta M_{A'} &= +2\delta\sqrt{1 - \tfrac{1}{2}\sin(2\theta)} \\ \delta M_{B'} &= -2\delta\sqrt{1 - \tfrac{1}{2}\sin(2\theta)} \\ \delta M_C &= \delta\left[\cos(\theta) - 2\sin(\theta)\right] \\ \delta M_D &= \delta\left[\cos(\theta) + \sin(\theta)\right] \\ \delta M_F &= \delta\left[\sin(\theta) - 2\cos(\theta)\right] \end{aligned} \tag{66}$$

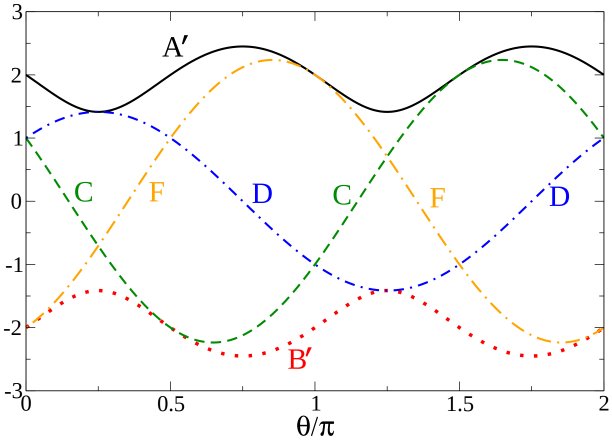

FIG. 16: Spectrum of quintuplet states as a function of θ which parametrizes gauge boson splittings. Units of δM_i are $2\sqrt{2}\alpha[(\mu_1-\mu_2)^2+(\mu_3-\mu_2)^2]^{1/2}$.

The spectrum as a function of θ is shown in fig. 16. The complete range of possibilities for splitting by radiative corrections alone is thus encompassed in the figure, assuming given values of the μ_i can be achieved by the appropriate choice of scalar VEV's.

B. Gauge interactions and mass hierarchies

The interactions of the gauge bosons with the quintuplet states are off-diagonal, as expected for Majorana particles. Suppressing Lorentz indices and gamma matrices, they are proportional to

$$\begin{aligned}\mathcal{L}_{\rm gauge} \sim\ & B_1(DC+\sqrt{3}FB+FA)+B_2(2AD-FC)\\ & +B_3(CA+\sqrt{3}BC+FD)\end{aligned} \qquad (67)$$

The transitions which can be mediated are shown in figure 6. This diagram is useful for determining what kinds of DM mass spectra can be consistent with explaining the various experimental observations.

1. *Inverted hierarchy and Z_2 symmetry*

Here we give some examples of the inverted mass hierarchy with Z_2 symmetry which can help boost the production of low-energy positrons as observed by INTEGRAL/SPI. In section IV C we identified the possible discrete symmetries which could exist for a given choice of gauge kinetic mixing. Consider the case where B_3 mixes with hypercharge. According to the arguments in section IV C, either D or F should be chosen as the intermediate state. Fig 16 shows that at $\theta \lesssim \pi/4$ F can be the stable intermediate state with a small mass gap below C. Scattering processes $FF\to CC$ in the galaxy can be enhanced, followed by $C\to B'e^+e^-$ via B_3 exchange. Similarly, at $\theta\gtrsim\pi$, D can be chosen as the intermediate state, giving rise to $DD\to CC$ followed by $C\to B'e^+e^-$. Both of these examples have analogous counterparts just on the other side of the degeneracy between states. At $\theta\gtrsim\pi/4$, the roles of C, F and B_1, B_3 are interchanged, while for $\theta\lesssim\pi$, the roles of C, D and B_2, B_3 are interchanged.

From fig. 16 we identify several other possible inverted hierarchy realizations: $\theta\cong 0$, with C, D as the topmost relevant states, $\theta\cong\pi/2$, involving D, F and $\theta\cong 5\pi/8$, involving C, F, and $\theta\cong 3\pi/2$ with D, F. In short, near every place where two mass eigenvalues cross at an angle, one can have an inverted mass hierarchy. There are six such values of θ where this occurs.

2. *Normal hierarchy*

If one prefers a model with normal mass hierarchy, fig. 16 shows that there are several possibilities, close to points where the B' curve is tangent to that of C, D or F. These occur at $\theta = 0,\ \pi/2,\ 5\pi/4$. Notice that very small mass splittings can be arranged near these points with relatively little tuning of θ due to the fact that the curves are tangent to each other. This gives another way of obtaining smaller splittings than the generic size.

Curiously, in no case can the heaviest state A' be relevant for XDM, because there is no gauge interaction which couples it to the lightest state B'. Instead A' is a spectator, and the highest relevant state is either C, D, F, one of which happens to be degenerate with A' at the angles $\theta=\pi/4$, π or $3\pi/2$.

3. *No combined hierarchy*

Because of the extra complexity of the quintuplet spectrum and gauge couplings, it is tempting to look for a situation where both the normal and the inverted hierarchies could exist simultaneously, combining the advantages of the latter for XDM while still leaving open an iDM explanation for DAMA. This turns out to be impossible, however. First consider the situation where only one gauge boson mixes with the SM, say B_1. To be compatible with both iDM and XDM, B_1 would have to mediate transitions between the ground state B', an admixture of A and B, and two other states. Perusal of the transitions in figure 6 shows that no gauge boson has this property.

The next alternative is that there are two gauge bosons which mix with the SM, one for the iDM transition and one for the XDM. The problem here is that then Z_2 symmetry is broken for two gauge bosons. The $B_1B_2B_3$ gauge interaction then forces it to be broken for all of them, and no Z_2 exists to protect the higher intermediate state for XDM from decaying.

IX. AN SU(2)×U(1) MODEL

A. Motivation

Most of the models described above have the advantage of allowing for the inverse hierarchy of mass splittings which can enhance the galactic 511 keV signal seen by INTEGRAL; however this comes at the expense of a nonthermal history for the DM in order to keep the intermediate mass state from being depopulated in the early universe. Furthermore, purely SU(2) DM models do not allow for the excitation $\chi_1\chi_1 \to \chi_2\chi_3$ which would have half the energy requirement of $\chi_1\chi_1 \to \chi_3\chi_3$. In the former case, one need only produce a single e^+e^- pair (if M_2 is only slightly above M_1), while in the latter, there must be at least enough energy for two pairs, and the excitation rate is therefore suppressed by the lack of sufficiently energetic DM particles in the galactic center. On the other hand, models with an extra U(1) in the dark gauge sector can have $\chi_1\chi_1 \to \chi_2\chi_3$ by virtue of mixing between the gauge groups when they are spontaneously broken.

Even the simplest SU(2)×U(1) model is considerably more complicated than most of the pure SU(2) examples. First, the DM is necessarily vector-like (Dirac), in order to have a large bare mass while carrying the extra U(1) charge, but the Dirac states must be split into Majorana states by the Higgs which spontaneously breaks the U(1). Furthermore, the gauge group must be completely broken, unlike the standard model where SU(2)×U(1) breaks to $U(1)$. Following [75] we refer to this extra requirement as "charge breaking." Custodial symmetry needs to also be broken in order for the excited DM states to be able to decay into SM particles, since otherwise the gauge bosons can be paired up into charged states such as $W^\pm = \sqrt{1/2}(B_1 \pm iB_2)$, analogous to the W bosons of the SM. This charge is conserved if custodial symmetry is unbroken [the "charge breaking" mentioned above only insures that there is no unbroken U(1)], which would prevent the transitions between similarly charged χ states needed by the XDM and iDM mechanisms. Here we will analyze in some detail a model of triplet SU(2)×U(1) DM with these necessary properties, which was outlined in ref. [75]. The potential needed for getting the desired pattern of Higgs VEVs is presented there.

B. Specification of the model

Consider two Weyl triplets χ_i and χ_i' which have equal and opposite dark hypercharge $\pm y'/2$. They can be given the bare mass term $M\chi_i\chi_i'$. Once the gauge symmetry is broken, mass splittings can arise both through radiative corrections and through Yukawa couplings to Higgs fields which acquire VEV's. We will assume that the radiative corrections dominate the mass splittings which respect $\chi{-}\chi'$ number conservation (the Dirac mass terms), while the Yukawa couplings (see (69) below) are responsible for splitting the degenerate Dirac states into Majorana ones.

To compute the radiative corrections, we must first find the spectrum of gauge bosons. As shown in ref. [75], complete breaking of SU(2)×U(1) requires two Higgs doublets with equal and opposite dark hypercharges $\pm y$, whose VEV's take the form

$$h_1 = v_1 \begin{pmatrix} \cos\alpha \\ \sin\alpha \end{pmatrix}, \quad h_2 = v_2 \begin{pmatrix} 0 \\ 1 \end{pmatrix} \qquad (68)$$

For convenience we will also include a triplet Higgs field Δ_i with VEV $\langle\Delta_i\rangle = \Delta\delta_{i1}$. This breaks the custodial symmetry at tree level. Without the triplet, custodial symmetry breaking first appears at one loop. To avoid the extra effort of computing loop effects, we parametrize the symmetry breaking using the triplet VEV. Finally, it is necessary to include a Higgs field ϕ with dark hypercharge $-y'$ which can split the Dirac components of the DM states, so that there are no diagonal DM couplings of the U(1) which mixes with SM hypercharge; such couplings are strongly constrained by direct DM searches, as discussed in section III B. The Yukawa couplings which accomplish this are

$$h\phi\chi_i\chi_i + h'\phi^*\chi_i'\chi_i' \qquad (69)$$

C. Mass eigenstates

The VEV's of the four Higgs fields h_i, Δ, ϕ give rise to the gauge boson mass matrix in the basis B_1, B_2, B_3, Y

$$\begin{pmatrix} A & 0 & 0 & gys_{2\alpha}v_1^2 \\ 0 & A+\delta & 0 & 0 \\ 0 & 0 & A+\delta & gy(c_{2\alpha}v_1^2+v_2^2) \\ gys_{2\alpha}v_1^2 & 0 & gy(c_{2\alpha}v_1^2+v_2^2) & B \end{pmatrix} \qquad (70)$$

where $A = g^2v^2$, $B = y^2v^2 + y'^2\phi^2$, $v^2 = v_1^2 + v_2^2$, $c_{2\alpha} = \cos 2\alpha$, $s_{2\alpha} = \sin 2\alpha$, $\delta = g^2\Delta^2$ and ϕ represents the VEV of the U(1)-breaking Higgs field in (69). In order to give analytic expressions, we will consider the off-diagonal charge-breaking elements to be small perturbations ϵ_i, and the custodial breaking to be even smaller, $\delta < \sum_i \epsilon_i^2/|A-B|$.

The diagonalization of (70) is worked out in appendix E. The masses eigenvalues of the four gauge bosons are given in eqs. (E10) and the mixings in eq. (E11). The standard model couplings induced by the mixing term $\epsilon Y_{\mu\nu}Y_{SM}^{\mu\nu}$ and the rotation matrix (E11) thus involve the mass eigenstates B_1', B_3', Y', while B_2 remains uncoupled to the SM currents. As a result, all the gauge bosons except B_2 have relative short lifetimes due to the decay into e^+e^-. We come back to the decays of B_2 below.

The aforementioned gauge interactions give rise to radiative corrections to the Dirac masses of the form $\sum_i \chi_i\delta M_i\chi_i'$. Only the SU(2) gauge interaction vertices contribute to the splittings, because the hypercharge interactions give equal contributions to each δM_i. Relating the flavor eigenstates B_i in terms of the mass eigenstates

B'_a by $B_i = R_{ia} B'_a$, and denoting $B'_4 = Y'$, the contributions to the δM_i are

$$\begin{aligned} \delta M_1 &= -\frac{1}{2}\alpha_g \left(\mu_2 + \sum_i R_{3i}^2 \mu_i \right) \\ \delta M_2 &= -\frac{1}{2}\alpha_g \sum_i \left(R_{1i}^2 + R_{3i}^2 \right) \mu_i \\ \delta M_3 &= -\frac{1}{2}\alpha_g \left(\mu_2 + \sum_i R_{1i}^2 \mu_i \right) \qquad (71) \end{aligned}$$

The coefficients R_{ia} are given in eq. (E11). Ignoring terms of $O(\delta^2)$, and subtracting the δM_3 contribution from all δM_i (since we are only interested in mass differences) we obtain

$$\begin{aligned} \delta M_1 &= \frac{1}{4}\alpha_g \left(\frac{s_\theta^2 \delta}{\sqrt{A}} - \epsilon^2 f(A,B) \right) \\ \delta M_2 &= \frac{1}{4}\alpha_g \left(\frac{\delta}{\sqrt{A}} - 2\psi^2\sqrt{A} - \epsilon^2 f(A,B) \right) \\ \delta M_3 &\equiv 0 \qquad (72) \end{aligned}$$

where $\epsilon = \sqrt{\epsilon_1^2 + \epsilon_2^2}$, $\tan\theta = \epsilon_1/\epsilon_2$, $f(A,B) = 2\sqrt{B}(A-B)^{-2} + [\sqrt{A}(A-B)]^{-1}$, and $\psi = c_\theta s_\theta (A-B)\delta/\epsilon^2$. One can show that the function $f(A,B)$ is positive for all values of A, B. Since we have assumed that $\delta \ll \epsilon^2/|A-B|$, this gives a normal hierarchy with $M_1 \sim M_2 < M_3$. Whether χ_1 or χ_2 is the lightest state depends on the ψ^2 term in δM_2. It is of order δ^2/ϵ^4, which can compete with the order δ term since only δ/ϵ^2 need be small for the consistency of our approximations.

The above mass splittings refer to Dirac states in the absence of the Majorana masses induced by (69) due to the VEV of ϕ. The effect of the latter is to split the Dirac mass eigenvalues by $\pm\frac{1}{2}(h+h')\langle\phi\rangle$. Thus we get two sets of states whose mass splittings are given by (72), but they are offset from each other by $m = (h+h')\langle\phi\rangle$. It would be consistent with our approximations to consider $m \gg \delta M_i$, so that the more massive set of states does not play any role at late times.

D. Phenomenology

It is interesting that the mass splittings (72) are parametrically suppressed to smaller values than the generic $\alpha_g \mu$ estimate, and that the hierarchy between custodial symmetry breaking and charge breaking, δ/ϵ^2, translates into the hierarchy of masses $M_1 \sim M_2 < M_3$, *i.e.,* it explains why one mass splitting should be parametrically smaller than the other. In terms of the model parameters, the smallness of ϵ_i can be arranged by assuming $y \ll g$, *i.e.,* the dark hypercharge of the Higgs doublets is much smaller than the SU(2) gauge coupling. The even smaller breaking of custodial symmetry seems to require an unnaturally small triplet VEV Δ in our implementation, but as mentioned above, this is only a crutch to avoid loop computations, since custodial symmetry is violated by hypercharge interactions even without the triplet. Because of the loop suppression on top of the small y coupling, this effect is indeed expected to be smaller than the charge breaking.

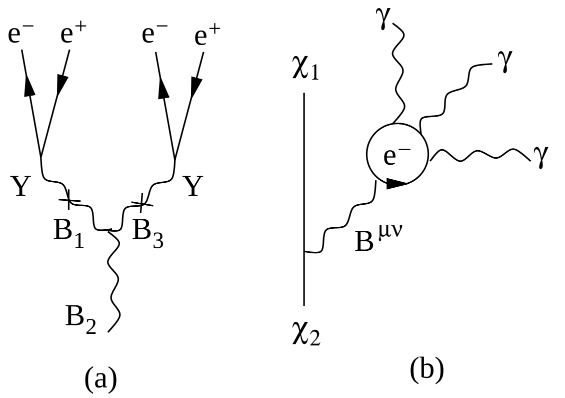

FIG. 17: (a) Left: diagram for $B_2 \to 4e$ decay. (b) Right: diagram for $\chi_2 \to \chi_1 + 3\gamma$ decay.

Another striking point is that B_2 is the only nonabelian gauge boson which has no mixing with Y, due to the form of the mass matrix (70), hence neither does B_2 mix with the SM hypercharge (however B_2 does decay into electrons via the process shown in fig. 17(a)). This means the transition between χ_1 and χ_3 is the only one that does not couple to the electron current, while the $\chi_2 \leftrightarrow \chi_1$ and $\chi_2 \leftrightarrow \chi_3$ transitions do. The $\chi_1 \leftrightarrow \chi_2$ transition can thus be used for the iDM mechanism. Moreover, assuming χ_1 is the lightest state, $\chi_1\chi_1 \to \chi_3\chi_2$ (possible because of B_3-Y mixing) followed by $\chi_3 \to \chi_2 e^+e^-$ can realize the XDM scenario, if $\delta M_{32} = M_3 - M_2 > 2m_e$. The other possibility is that χ_2 is the lowest state, so that $\chi_2\chi_2 \to \chi_1\chi_3$ (enabled by B_3-B_1 mixing) is the excitation channel.

In the case where χ_1 is the ground state, we have the situation where χ_2 is a long-lived intermediate state whose transitions $\chi_2 \leftrightarrow \chi_{1,3}$ couple to currents involving nucleons or electrons. This situation is highly constrained by direct detection experiments, as we explained in section V F. Let us first show that χ_2 is cosmologically long-lived. The χ_2 state can decay to $\chi_1 + 3\gamma$ through the operator $\epsilon\alpha^2 m_e^{-4} B_3 F^3$ which is induced through a virtual electron loop, shown in fig. 17(b). Ref. [53] (see also [76]) estimated the rate to be

$$\Gamma(\chi_2 \to \chi_1 + 3\gamma) = \frac{17\epsilon^2\alpha_g\alpha^4(\delta M_{32})^{13}}{2^7 3^6 5^3 \pi^3\, m_e^8\, \mu^4} \qquad (73)$$

For the parameter values we have favored, $\epsilon = 10^{-3}$, $M_\chi = 1$ TeV, $\mu = 100$ MeV, $\delta M_{32} = 100$ keV, $\alpha_g = 0.04$, the lifetime is around 10^{21} s, much greater than the age of the universe. The constraint (44) thus applies. According to ref. [53], such small couplings are inconsistent with an iDM explananation of the DAMA observations. Thus the main potential advantage of this model over a simpler one, such as doublet DM, is the lower energy threshold excitation channel $\chi_1\chi_1 \to \chi_2\chi_3$ for XDM.

X. CONCLUSIONS

We have surveyed a range of experimental and cosmological constraints on the simplest models of dark matter with a hidden SU(2) gauge symmetry, with a view toward explaining the PAMELA, Fermi/LAT and INTEGRAL/SPI electron/positron excesses by DM annihilation or excitation. Although new constraints on inverse Compton gamma rays associated with the e^+e^- production are making it more difficult to accommodate the scenario, models like those we pinpoint where $M_\chi \cong 1$ TeV, $\alpha_g \sim 0.04$, the mass of the intermediate gauge or Higgs boson is $\lesssim 100$ MeV, and the annihilations proceed via $\chi\chi \to 4e$ rather than $2e$ or any combination of heavier leptons, seem to still be viable.

There are two uncertainties in the properties of DM halos which can help alleviate the constraints from gamma rays produced in our own galaxy. One is the possible presence of many subhalos with low velocity dispersion being the principal regions of dark matter annihilation would displace the gamma rays away from the galactic center, where constraints from HESS are strongest. The other arises from new studies of the effects of baryons on the DM velocity dispersion profiles, which imply that Sommerfeld-enhanced annihilation would be suppressed near the galactic center. These two effects could work together such that PAMELA/Fermi observations are dominated by subhalo annihilations, while the the 511 keV excess is enhanced by the larger DM velocities in the galactic center. We have ruled out a third possibility in the present class of models, namely that the intermediate particles decaying into e^+e^- travel away from the galactic center before decaying; we showed that such particles would necessarily spoil BBN because of their long lifetimes and high abundance in the early universe.

All of these loopholes are relatively unimportant for a related class of constraints, which considers the gamma rays emitted by all halos at all redshifts, including their effect on the CMB. It would be important to reconsider these constraints specifically for annihilations in which $\chi\chi \to 4e$, and higher numbers of electrons/positrons, due to cascading of the dark gauge bosons, to see how much they really constrain the present class of models.

We have shown that there is a new potential signal which could provide additional evidence for nonabelian DM, if the XDM interpretation of the INTEGRAL 511 keV excess is correct. The DM transition magnetic moment interaction induced at one loop, due to the nonabelian terms in the gauge kinetic mixing, should give rise to a narrow gamma ray line with energy equal to the mass splitting of the two DM states, expected to be of order a few MeV. Our estimates show that for $\alpha_g \sim 0.04$, the strength of this line can be close to the current sensitivity of INTEGRAL/SPI, if the phase space for excited dark matter decay is accidentally small.

Another potential signal is through the couplings of the portal particle which interacts with the SM, with coupling reduced by the factor ϵ if it is a dark gauge boson, or mixing angle θ if it is a Higgs boson. The ϵ factor is already strongly constrained, depending on the mass μ of the portal boson, by precision QED tests and beam dump experiments. Proposed fixed target experiments could further probe the allowed range of ϵ in the near future. We have derived the bound $\epsilon \gtrsim 4 \times 10^{-11}$ in the case of gauge kinetic mixing, from the requirement that dark gauge bosons annihilate to e^+e^- efficiently before nucleosynthesis. If any of the gauge bosons are stable, we get the stronger bound $\epsilon \gtrsim 3 \times 10^{-10}$ from overclosure. This is three orders of magnitude smaller than current limits from the E137 beam dump experiment. In the case of Higgs mixing, we find an analogous lower bound $\theta \gtrsim 10^{-6}$ on the Higgs mixing angle.

We have also shown that Higgs mixing rather than gauge kinetic mixing can be a viable portal to the SM, despite first appearances that it would tend to induce too high a rate of $\chi_i\chi_i \to f\bar{f}$, where f is any SM fermion, preferably the top quark. Such diagonal couplings of the Higgs to $\chi_i\chi_i$ might also be expected to lead to too high of a cross section for scattering from nucleons, $\chi N \to \chi N'$, in direct DM detectors. We have shown that in fact the constraints can easily be satisfied for reasonable values of the couplings.

Concerning specific models, the simplest possibility is DM in the doublet representation, which has the potential for implementing the XDM mechanism to explain INTEGRAL/SPI observations of 511 keV gamma rays from the galactic center. We noted that the doublet model must get its mass splitting from a Yukawa coupling to a triplet Higgs, rather than from radiative corrections, which divorces the scale of the mass splitting from the strength of the gauge coupling.

A recurring theme of our paper was the possibility of an inverted mass hierarchy in models with three or more DM components, which can help boost the production of the 511 keV excess by the XDM mechanism. A Z_2 discrete symmetry is required to keep the intermediate-mass DM state stable in this scenario. We showed that models of triplet and quintuplet DM afford many examples with the desired properties, as well as the alternative normal mass hierarchy. In both triplet and quintuplet DM models, it is possible to choose Higgs VEVs such that the mass splittings are smaller than the generic estimate $\alpha_g\mu$ for the size of the radiative corrections, which can be help explain the hierarchy between splittings needed for the iDM or inverse mass hierarchy XDM scenarios. An in-depth reanalysis of the viability of the XDM mechanism for explaining the 511 keV observation, in the context of the present class of models, is in progress [69].

We have not focused on the DAMA/LIBRA annual modulation as one of the signals to be explained by nonabelian dark matter, even though that was cited as one of the original motivations for this class of models. Our choice stems from recent results [52] which note that the iDM explanation for the signal is ruled out at the 99% c.l. by data from the ZEPLIN-II and at 95% c.l. by XENON10 and CRESST II observations, for DM whose mass is in the range of interest for explaining the PAMELA/Fermi lepton excesses. Another reason is that our proposal of the inverted mass hierarchy for boosting the XDM mechanism is at odds with the normal mass hierarchy needed for iDM. However if one believes there is still room for iDM to work, then the desired mass splittings can be achieved within the models considered here (for DM in triplet and higher representations), since there is great freedom to adjust the DM spectra through ratios of the VEV's of the dark Higgs fields.

In summary, SU(2) gauge theories of DM continue to offer an elegant explanation for numerous effects, with intricate implications for cosmology, DM halo properties, laboratory tests, and the prospect for being ruled in or out in the near future.

Acknoweldgment. We thank Sabine Kraml for assistance with MicrOMEGAs, Guy Moore for information about the Higgs-nucleon coupling, Emiliano Mocchiutti for correspondence about the PAMELA antiproton background, Julio Navarro for discussions on the effect of baryons on DM halos, Maxim Pospelov for discussions about long-lived intermediate states, Andrew Strong for valuable advice about the interpretation of INTEGRAL/SPI data, and Aaron Vincent for discussions about GALPROP. Our work is supported by NSERC of Canada.

APPENDIX A: TRANSITION MAGNETIC MOMENT

By routing the external momenta through the loop in the appropriate way, the expression for the loop diagram which gives rise to the transition magnetic moment can be written as

$$\int \frac{d^4p}{(2\pi)^4} \frac{\epsilon g^3\, \gamma_\mu(\not{p} + \not{\bar{q}} + M_1)\gamma_\nu}{[(p+\bar{q})^2 - M_1^2][(p+\delta q)^2 - \mu^2][(p-\delta q)^2 - \mu^2]} \tag{A1}$$

antisymmetrized over μ, ν (since it is contracted with $F_{\mu\nu}$ of the external photon), where $\bar{q}$ is the average 4-momentum of the two external DM states, $\bar{q} = \frac{1}{2}(q_3 + q_2)$, and δq is half the 4-momentum of the photon, $\delta q = \frac{1}{2}(q_3 - q_2)$, and M_1 is the mass of the virtual DM particle. We have ignored mass differences between the two gauge bosons in the loop since this has a subleading effect on the result. Using Feynman parameters and Wick rotating, the p integral can be done, leading to

$$\epsilon g^3 \int_0^1 dx \int_0^{1-x} dy \tag{A2}$$
$$\frac{\gamma_\mu((x+y)\not{\bar{q}} + (y-x)\delta\not{q} + M_1)\gamma_\nu}{z^2M^2 + \frac{1}{2}(y-x)z\delta M_{32}^2 + \delta M_{123}^2 z + \mu^2(x+y)}$$

where $z = 1 - x - y$, $\delta M_{123}^2 = M_1^2 - \frac{1}{2}(M_2^2 + M_3^2)$, and $\delta M_{32}^2 = M_3^2 - M_2^2$. For the parameter values of interest, we find that it is a good approximation to set $\delta M_{32}^2 = \delta M_{123}^2 = 0$ in the denominator. By anticommuting gamma matrices in the numerator and using the Dirac equation for the external spinors, one can show that $\not{\bar{q}} \to -\frac{1}{2}(M_2 + M_3)$, while $\delta\not{q}$ gives a subleading in δM_{23} contribution which can be neglected. Furthermore, it is a good approximation to set $(x+y) = 1$ for the coefficient of μ^2 in the denominator. In this way one can get the analytic approximation (11), which we have numerically verified to be good in the range of parameters of interest.

APPENDIX B: RADIATIVE DM MASS SPLITTINGS

In this appendix we present the radiative mass corrections to a DM multiplet χ_i by virtual massive gauge bosons, as shown in fig. 5(a). Assume the DM multiplet transforms under a gauge group G with generators T_j. Also assume the gauge bosons A_j have mass μ_j. Figure 5(a) gives a correction to the self-energy of χ_i of

$$\delta M_i = g^2 \sum_{j,a} T^j_{ia} T^j_{ai} \int_0^1 dx \int \frac{d^4k_E}{(2\pi)^4} \frac{4M_a - 2\not{p}x}{(k_E^2 + \Delta)^2} \tag{B1}$$

where $\Delta = -M_i^2(1-x)x + \mu_j^2 x + M_a^2(1-x) \simeq M_a^2(1-x)^2 + \mu_j^2 x$. After integrating over the Euclidean 4-momentum k_E and using the equation of motion to set $\not{p} \to M_i$, we find two pieces, one of which is ultraviolet (UV) divergent, while the other is infrared (IR) divergent as $\mu_j \to 0$,

$$\delta M_i = \frac{g^2}{8\pi^2} \sum_{j,a} T^j_{ia} T^j_{ai} \int_0^1 dx\, (2M_a - M_i x)\, (\ln\Lambda^2 - \ln\Delta) \tag{B2}$$

where Λ is the ultraviolet cutoff of k_E. We are only interested in the IR divergent term because the UV divergent term cancels out when considering mass splittings. Notice that the IR divergence occurs when $x \to 1$, so we can set $x = 1$ in the first factor of the integrand.

Further assuming that the gauge boson mass is much smaller than the DM mass, $\mu_j \ll M_a$, and ignoring the χ mass splittings on the r.h.s., the IR divergent term turns out to be

$$\begin{aligned} \delta M_i &= -\frac{\alpha}{2\pi} M_\chi \sum_{j,a} T^j_{ia} T^j_{ai} \int_0^1 dx \\ &\quad \left(\ln\left(1 + \frac{x\mu_j^2}{(1-x)^2 M_\chi^2}\right) + 2\ln\left((1-x)M_\chi\right) \right) \\ &\to -\frac{\alpha}{2} \sum_{j,a} \mu_j T^j_{ia} T^j_{ai} \end{aligned} \tag{B3}$$

We dropped the last term because it is the same for each component of the DM multiplet and thus has no effect on the mass splitting.

Now we turn to the mass correction from virtual Higgs bosons. For illustration, suppose we have triplet DM χ_i coupled to a quintuplet scalar S_{ij}, via $h_s \chi_i S_{ij} \chi_j$. This induces radiative mass corrections through the diagram of fig. 5(b). Similarly to the gauge boson case we have,

$$\begin{aligned}\delta M_i &= \frac{\alpha_h}{4\pi}\sum_j M_j \int_0^1 dx \\ &\quad \left(\ln\left(1+\frac{x\, m_{ij}^2}{(1-x)^2 M_j^2}\right) + 2\ln\left((1-x)M_j\right)\right) \\ &\to \frac{\alpha_h}{4}\sum_j m_{ij} \qquad \text{(B4)}\end{aligned}$$

where the last approximation applies if the dark Higgs boson mass is much smaller than the dark matter mass, $m_{ij} \ll M_a$.

APPENDIX C: DM ANNIHILATION CROSS SECTION

Here we derive the annihilation cross sections for DM in the doublet, triplet and quintuplet representations. Because of its relative simplicity we start with the triplet case, assuming Majorana DM, whose gauge interaction Lagrangian is

$$\mathcal{L}_{\rm int} = \frac{1}{2}\, g\, \epsilon_{abc}\, \bar\chi_a B^b_\mu \gamma^\mu \chi_c \qquad \text{(C1)}$$

For the annihilation channel $\chi_1\chi_1 \to B_2 B_2$, the relevant interaction is

$$g \bar\chi_1 B_2^\mu \gamma_\mu \chi_3 \qquad \text{(C2)}$$

where the antisymmetric property of the Majorana vector current, $\bar\chi_3\gamma^\mu\chi_1 = -\bar\chi_1\gamma^\mu\chi_3$ has been used. The matrix element for $\chi_1\chi_1 \to B_2 B_2$ is then

$$\begin{aligned}\mathcal{M}_{11} &= -ig^2 \bar v(p_1) \not\epsilon(q_1) \frac{1}{\not p_1 - \not q_1 - M_\chi} \not\epsilon(q_2) u(p_2) \\ &\quad -ig^2 \bar v(p_1) \not\epsilon(q_2) \frac{1}{\not p_1 - \not q_2 - M_\chi} \not\epsilon(q_1) u(p_2) \qquad \text{(C3)}\end{aligned}$$

where p_i are the incoming χ momenta and q_i are the outgoing B momenta, and the ϵ's are polarization vectors. This has algebraically the same form as the matrix element for electron-positron annihilation. In the nonrelativistic and $M_\chi \gg \mu$ limits, the spin-averaged squared matrix element is $2g^4$ for both the t and u channels squared. The interference term vanishes in these limits. The sum over final states includes $\chi_1\chi_1 \to B_3 B_3$ as well, so the total is $8g^4$.

Next we consider the $\chi_1\chi_2 \to B_1 B_2$, which procedes by a sum of t-channel mediated by internal χ_3 and s-channel mediated by B_3 (using the 3-gauge boson vertex). The matrix element is

$$\begin{aligned}\mathcal{M}_{12} &= -ig^2 \bar v(p_1) \not\epsilon(q_1) \frac{1}{\not p_1 - \not q_1 - M_\chi} \not\epsilon(q_2) u(p_2) \\ &- ig^2 \frac{\bar v(p_1)\gamma_\nu u(p_2)}{p_s^2 - \mu^2} \left[\eta_{\nu\lambda}(p_s + q_2)_\mu \right.\\ &\qquad \left. -\eta_{\nu\mu}(p_s+q_1)_\lambda + \eta_{\mu\lambda}(q_1 - q_2)_\nu\right] \qquad \text{(C4)}\end{aligned}$$

where $p_s = p_1 + p_2$. We find that the spin-averaged squared matrix element gets contributions of $2g^4$, $-(19/4)g^4$ and $4g^4$ from the t^2, s^2 and interference channels, respectively, in the same limits as mentioned above. (The fact that the direct s^2 term is negative is due to the unphysical polarizations in the sum over final state gauge bosons; only the full amplitude squared is physically meaningful.) The total is thus $(5/4)g^4$.

Finally we must average over the initial colors to give $\langle|\mathcal{M}^2|\rangle = \frac{1}{3}\mathcal{M}_{11}^2 + \frac{2}{3}\mathcal{M}_{12}^2 = [8/3 + (2/3)(5/4)]g^4 = (7/2)g^4$. This must be multiplied by an additional factor of 1/2 for the indistinguishability of the final states. The differential cross section is thus

$$\frac{d\sigma}{dt} = \frac{(7/4)g^4}{64\pi s M_\chi^2 v^2} \qquad \text{(C5)}$$

evaluated in the center of mass frame. Integrating over the range of the Mandelstam t variable $\delta t = 4M^2 v$ and using the relative velocity $v_{\rm rel} = 2v$, we obtain the cross section (34) for the triplet case.

To find the annihilation cross section for DM in other representations, we work out the group theory factors for the general case. For the t^2 and u^2 terms, these take the form $(1/d_R^2)\sum_{ab}{\rm tr}(T^aT^aT^bT^b) = C_2(R)^2/d_R$, where $d_R = 2j+1$ is the dimension of the spin j representation and $C_2(R) = j(j+1)$ is the quadratic Casimir invariant. The factors $(1/d_R^2)$ come from averaging over the colors of the initial states. For the s^2 term we get $(1/d_R^2)\sum_{ij}\sum_{abcd}\epsilon^{abc}\epsilon^{abd}T^c_{ij}(T^d_{ij})^* = 2/d_R^2\sum_c {\rm tr}[T^cT^c] = 2C_2(R)/d_R$. For the st term, we find $(1/d_R^2){\rm tr}(T^aT^bT^c)\epsilon_{abc} = (i/2d_R^2)\epsilon_{abd}\epsilon_{abc}{\rm tr}(T^dT^c) \sim C_2(R)/d_R$.

Using these results, we can generalize the triplet computation to other representations. Using t^2, u^2, s^2 and st to represent the contribution to the squared matrix element from any definite external states (hence encoding the spin sums but not the group theory factors) we have

$$\langle|\mathcal{M}^2|\rangle = \frac{2}{3}\left(\frac{3}{2}(t^2+u^2) + s^2 + st\right) \qquad \text{(C6)}$$

in the triplet representation, which based on the above group theory factors, generalizes to

$$\frac{2}{3}\frac{3}{d_R}\left(\frac{3}{2}\left(\frac{C_2(R)}{2}\right)^2(t^2+u^2) + \frac{C_2(R)}{2}(s^2+st)\right) \qquad \text{(C7)}$$

where $t^2 = u^2 = 2g^4$, $s^2 = -(19/4)g^4$ and $st = 4g^4$. We obtain

$$\langle|\mathcal{M}^2|\rangle = \frac{3j(j+1)}{2j+1}\left[j(j+1) - \frac{1}{4}\right] g^4 \qquad \text{(C8)}$$

for the spin-j representation. This must still be multiplied by the symmetry factor 1/2 for identical final states.

APPENDIX D: RATE OF $3B\to 2B$ DOWN-SCATTERING PROCESS

In the case of $\epsilon \ll 1$ where dark gauge bosons do not stay in kinetic equilibrium with the SM particles, the processes which can delay them from dominating the energy density of the universe after becoming nonrelativistic are those which convert 3 to 2 particles. The squared matrix element for $3B\to 2B$ in nonabelian gauge theory is of order $|\mathcal{M}|^2 \sim g^6/\mu^2$ if the B's are nonrelativistic. The Boltzmann equation for the number density of B's takes the form $\dot n_B + 3Hn_B = \mathcal{C}$. The collision term of interest for $3B\to 2B$ is

$$\begin{aligned}\mathcal{C} &\sim -\int\prod_i \frac{3\,d^3p_i}{(2\pi)^3 2E_i} f_1 f_2 f_3 |\mathcal{M}|^2 \\ &\times\; (2\pi)^4\delta^{(4)}(p_1+p_2+p_3-p_4-p_5) \\ &\cong \frac{n_B^3(T)(3/2)^5(4\pi)^4}{(2\pi)^{11}\mu^3}\frac{g^6}{\mu^2} \end{aligned}\qquad\text{(D1)}$$

where the nonrelativistic density is $n_B(T) = (\mu T)^{3/2}e^{-\mu/T}$. To convert this to a rate, we should divide by one power of n_B. Equating this to the Hubble rate, we find that

$$2x_f = \ln\left(\frac{3.4\alpha_g^3 M_p}{\mu}\right) - \ln x_f \qquad\text{(D2)}$$

leading to the result in the text above eq. (40).

APPENDIX E: DIAGONALIZATION OF SU(2)×U(1) MODEL MASS MATRICES

We give the details of approximately solving for the mass eigenvalues and eigenstates in the SU(2)×$U(1)$ DM model discussed in section IX. The dark gauge bosons are denoted by B_i and Y, and the effects of mixing with the SM hypercharge are neglected in the following approximations. Since B_2 does not mix with the other fields, we can consider the nontrivial 3×3 mass matrix in the B_1, B_3, Y basis, writing it in the form

$$\mu^2 = \begin{pmatrix} \bar A & \epsilon \\ \epsilon^t & B\end{pmatrix} \qquad\text{(E1)}$$

where $\bar A = \mathrm{diag}(g^2v^2, g^2v^2+\delta)$

$$\epsilon = gy\begin{pmatrix} s_{2\alpha}v_1^2 \\ c_{2\alpha}v_1^2 + v_2^2\end{pmatrix} = \begin{pmatrix}\epsilon_1\\ \epsilon_2\end{pmatrix} \qquad\text{(E2)}$$

and $B = y^2v^2 + y'^2\phi^2$. It is convenient to change bases using a global SU(2) rotation which makes only the lower component of ϵ nonzero. This is accomplished using a 2×2 rotation $R(\theta)$ in the B_1-B_3 subspace, with $\tan\theta = \epsilon_1/\epsilon_2$. In the new basis, $\bar A$ is no longer diagonal,

$$\bar A \to g^2v^2\mathbf{1} + \delta\begin{pmatrix} s_\theta^2 & c_\theta s_\theta \\ c_\theta s_\theta & c_\theta^2\end{pmatrix} \qquad\text{(E3)}$$

where $s_\theta = \sin\theta$, $c_\theta = \cos\theta$, and $\mathbf{1}$ is the 2×2 unit matrix Treating ϵ as a perturbation, one can perform a 3×3 rotation to get rid of the off-diagonal ϵ blocks, using

$$O = \begin{pmatrix} \mathbf{1} - \eta\eta^t/2 & -\eta \\ \eta^t & 1-\eta^t\eta/2\end{pmatrix} \qquad\text{(E4)}$$

where $\eta = (\bar A - B\times\mathbf{1})^{-1}\epsilon \equiv \tilde A^{-1}\epsilon$. Under this rotation, the 2×2 block $\bar A$ transforms again, receiving a correction $\bar A \to \bar A + \delta\bar A$ of the form

$$\delta\bar A = -\frac{1}{2}\{\bar A, \tilde A^{-1}X\tilde A^{-1}\} + \{X, \tilde A^{-1}\} + B\tilde A^{-1}X\tilde A^{-1} \qquad\text{(E5)}$$

where X is the 2×2 matrix $\epsilon\epsilon^t$, whose only nonvanishing component is ϵ^2 in the 2,2 position. We find that to leading order in δ,

$$\delta\bar A = \left(\begin{array}{c|c} 0 & -\frac{c_\theta s_\theta\delta\epsilon^2}{2(A-B)^2} \\ \hline -\frac{c_\theta s_\theta\delta\epsilon^2}{2(A-B)^2} & \frac{\epsilon^2}{A-B}\left(1 - \frac{c_\theta^2\delta}{2(A-B)}\right)\end{array}\right) \qquad\text{(E6)}$$

where $A = g^2v^2$. B gets a similar correction, but the correction to $\bar A$ is more important since this splits the gauge boson mass eigenvalues, whereas B is already well separated from the eigenvalues of the $\bar A$ matrix. The final step for the gauge boson mass eigenvalues is to diagonalize $\bar A + \delta\bar A$. The off-diagonal elements of $\delta\bar A$ give only $O(\delta^2)$ corrections to the gauge boson mass splittings, which we are ignoring; thus, denoting $A = g^2v^2$ and $B = y^2v^2 + y'^2\phi^2$, the resulting masses are

$$\begin{aligned} \mu_1^2 &= A + s_\theta^2\delta + O(\delta^2) &\text{(E7)}\\ \mu_2^2 &= A + \delta &\text{(E8)}\\ \mu_3^2 &= A + \frac{\epsilon^2}{A-B} + O(\delta) &\text{(E9)}\\ \mu_4^2 &\cong B &\text{(E10)}\end{aligned}$$

The relation between the flavor (unprimed) and mass (primed) eigenstates is $B_2 = B_2'$ and

$$\begin{pmatrix} B_1 \\ B_3 \\ Y\end{pmatrix} \cong \begin{pmatrix} 1 & \psi & 0 \\ -\psi & 1 & -\eta \\ -\eta\psi & \eta & 1\end{pmatrix}\begin{pmatrix} B_1' \\ B_3' \\ Y'\end{pmatrix} \qquad\text{(E11)}$$

where

$$\eta = \frac{\epsilon}{A+\delta-B},\quad \psi = c_\theta s_\theta(A-B)\frac{\delta}{\epsilon^2} \qquad\text{(E12)}$$

Here ψ is the small angle of the rotation which diagonalizes (E6). It gives rise to $O(\delta^2/\epsilon^4)$ contributions to the mass splittings of the DM states, which are larger than the $O(\delta^2)$ terms we have ignored thus far. These formulas assume $\delta < \epsilon^2/|A-B|$, so they are not valid in the limit $\epsilon\to 0$.

---

[1] N. Arkani-Hamed, D. P. Finkbeiner, T. R. Slatyer and N. Weiner, "A Theory of Dark Matter," Phys. Rev. D **79**, 015014 (2009) [arXiv:0810.0713 [hep-ph]].

[2] O. Adriani *et al.*, "Observation of an anomalous positron abundance in the cosmic radiation," arXiv:0810.4995 [astro-ph].

[3] J. Chang *et al.*, "An Excess Of Cosmic Ray Electrons At Energies Of 300.800 Gev," Nature **456** (2008) 362.

[4] S. Torii *et al.*, "High-energy electron observations by PPB-BETS flight in Antarctica," arXiv:0809.0760 [astro-ph].

[5] S. W. Barwick *et al.* [HEAT Collaboration], "Measurements of the cosmic-ray positron fraction from 1-GeV to 50-GeV," Astrophys. J. **482**, L191 (1997) [arXiv:astro-ph/9703192].

[6] J. Knödlseder *et al.*, "Early SPI/INTEGRAL contraints on the morphology of the 511 keV line emission in the 4th galactic quadrant," Astron. Astrophys. **411**, L457 (2003) [arXiv:astro-ph/0309442];
J. Knödlseder *et al.*, "The all-sky distribution of 511-keV electron positron annihilation emission," Astron. Astrophys. **441**, 513 (2005) [arXiv:astro-ph/0506026];
P. Jean *et al.*, "Early SPI/INTEGRAL measurements of galactic 511 keV line emission from positron annihilation," Astron. Astrophys. **407**, L55 (2003) [arXiv:astro-ph/0309484].

[7] D. P. Finkbeiner and N. Weiner, "Exciting Dark Matter and the INTEGRAL/SPI 511 keV signal," Phys. Rev. D **76**, 083519 (2007) [arXiv:astro-ph/0702587].

[8] R. Bernabei *et al.* [DAMA Collaboration], "First results from DAMA/LIBRA and the combined results with DAMA/NaI," Eur. Phys. J. C **56**, 333 (2008) [arXiv:0804.2741 [astro-ph]].

[9] D. Tucker-Smith and N. Weiner, "Inelastic dark matter," Phys. Rev. D **64**, 043502 (2001) [arXiv:hep-ph/0101138].
D. Tucker-Smith and N. Weiner, "The status of inelastic dark matter," Phys. Rev. D **72**, 063509 (2005) [arXiv:hep-ph/0402065].
S. Chang, G. D. Kribs, D. Tucker-Smith and N. Weiner, "Inelastic Dark Matter in Light of DAMA/LIBRA," arXiv:0807.2250 [hep-ph].
A. Menon, R. Morris, A. Pierce and N. Weiner, "Capture and Indirect Detection of Inelastic Dark Matter," arXiv:0905.1847 [hep-ph].

[10] D. P. Finkbeiner, "Microwave ISM Emission Observed by WMAP," Astrophys. J. **614**, 186 (2004) [arXiv:astro-ph/0311547];
D. P. Finkbeiner, "WMAP microwave emission interpreted as dark matter annihilation in the inner Galaxy," arXiv:astro-ph/0409027.
G. Dobler and D. P. Finkbeiner, "Extended Anomalous Foreground Emission in the WMAP 3-Year Data," Astrophys. J. **680**, 1222 (2008) [arXiv:0712.1038 [astro-ph]].
D. Hooper, D. P. Finkbeiner and G. Dobler, "Evidence Of Dark Matter Annihilations In The WMAP Haze," Phys. Rev. D **76**, 083012 (2007) [arXiv:0705.3655 [astro-ph]].

[11] A. A. Abdo *et al.* [The Fermi LAT Collaboration], "Measurement of the Cosmic Ray e+ plus e- spectrum from 20 GeV to 1 TeV with the Fermi Large Area Telescope," Phys. Rev. Lett. **102**, 181101 (2009) [arXiv:0905.0025 [astro-ph.HE]].

[12] F. Aharonian *et al.* [H.E.S.S. Collaboration], "The energy spectrum of cosmic-ray electrons at TeV energies," Phys. Rev. Lett. **101**, 261104 (2008) [arXiv:0811.3894 [astro-ph]];
"Probing the ATIC peak in the cosmic-ray electron spectrum with H.E.S.S," arXiv:0905.0105 [astro-ph.HE].

[13] T. Delahaye, R. Lineros, F. Donato, N. Fornengo and P. Salati, "Positrons from dark matter annihilation in the galactic halo: theoretical uncertainties," Phys. Rev. D **77**, 063527 (2008) [arXiv:0712.2312 [astro-ph]].

[14] M. Cirelli, M. Kadastik, M. Raidal and A. Strumia, "Model-independent implications of the e+, e-, anti-proton cosmic ray spectra on properties of Dark Matter," Nucl. Phys. B **813**, 1 (2009) [arXiv:0809.2409 [hep-ph]].

[15] A. Ibarra and D. Tran, "Decaying Dark Matter and the PAMELA Anomaly," JCAP **0902**, 021 (2009) [arXiv:0811.1555 [hep-ph]].

[16] P. f. Yin, Q. Yuan, J. Liu, J. Zhang, X. j. Bi and S. h. Zhu, "PAMELA data and leptonically decaying dark matter," Phys. Rev. D **79**, 023512 (2009) [arXiv:0811.0176 [hep-ph]].

[17] I. Cholis, D. P. Finkbeiner, L. Goodenough and N. Weiner, "The PAMELA Positron Excess from Annihilations into a Light Boson," arXiv:0810.5344 [astro-ph]. I. Cholis, G. Dobler, D. P. Finkbeiner, L. Goodenough and N. Weiner, "The Case for a 700+ GeV WIMP: Cosmic Ray Spectra from ATIC and PAMELA," arXiv:0811.3641 [astro-ph].

[18] P. Meade, M. Papucci and T. Volansky, "Dark Matter Sees The Light," arXiv:0901.2925 [hep-ph].

[19] J. Mardon, Y. Nomura, D. Stolarski and J. Thaler, "Dark Matter Signals from Cascade Annihilations," JCAP **0905**, 016 (2009) [arXiv:0901.2926 [hep-ph]].

[20] I. Z. Rothstein, T. Schwetz and J. Zupan, "Phenomenology of Dark Matter annihilation into a long-lived intermediate state," arXiv:0903.3116 [astro-ph.HE].

[21] K. Hamaguchi, K. Nakaji and E. Nakamura, "Inverse Problem of Cosmic-Ray Electron/Positron from Dark Matter," arXiv:0905.1574 [hep-ph].

[22] D. Malyshev, "On discrepancy between ATIC and Fermi data," arXiv:0905.2611 [astro-ph.HE].

[23] L. Bergstrom, J. Edsjo and G. Zaharijas, "Dark matter interpretation of recent electron and positron data," arXiv:0905.0333 [astro-ph.HE].

[24] C. Balazs, N. Sahu and A. Mazumdar, "Absolute electron and positron fluxes from PAMELA/Fermi and Dark Matter," arXiv:0905.4302 [hep-ph].

[25] P. Meade, M. Papucci, A. Strumia and T. Volansky, "Dark Matter Interpretations of the Electron/Positron Excesses after FERMI," arXiv:0905.0480 [hep-ph].

[26] J. Liu, Q. Yuan, X. Bi, H. Li and X. Zhang, "A Markov Chain Monte Carlo Study on Dark Matter Property Related to the Cosmic $e^{\pm}$ Excesses," arXiv:0906.3858 [astro-ph.CO].

[27] M. Cirelli, R. Franceschini and A. Strumia, "Minimal Dark Matter predictions for galactic positrons, anti-protons, photons," Nucl. Phys. B **800**, 204 (2008) [arXiv:0802.3378 [hep-ph]].
J. H. Huh, J. E. Kim and B. Kyae, "Two dark matter components in N_{DM}MSSM and PAMELA data," arXiv:0809.2601 [hep-ph].

M. Pospelov and A. Ritz, “Astrophysical Signatures of Secluded Dark Matter,” Phys. Lett. B **671**, 391 (2009) [arXiv:0810.1502 [hep-ph]].

J. Hisano, M. Kawasaki, K. Kohri and K. Nakayama, “Positron/Gamma-Ray Signatures of Dark Matter Annihilation and Big-Bang Nucleosynthesis,” Phys. Rev. D **79**, 063514 (2009) [arXiv:0810.1892 [hep-ph]].

A. E. Nelson and C. Spitzer, “Slightly Non-Minimal Dark Matter in PAMELA and ATIC,” arXiv:0810.5167 [hep-ph].

Y. Nomura and J. Thaler, “Dark Matter through the Axion Portal,” arXiv:0810.5397 [hep-ph].

R. Harnik and G. D. Kribs, “An Effective Theory of Dirac Dark Matter,” arXiv:0810.5557 [hep-ph].

D. Feldman, Z. Liu and P. Nath, “PAMELA Positron Excess as a Signal from the Hidden Sector,” Phys. Rev. D **79**, 063509 (2009) [arXiv:0810.5762 [hep-ph]].

K. Ishiwata, S. Matsumoto and T. Moroi, “Cosmic-Ray Positron from Superparticle Dark Matter and the PAMELA Anomaly,” Phys. Lett. B **675**, 446 (2009) [arXiv:0811.0250 [hep-ph]].

Y. Bai and Z. Han, “A Unified Dark Matter Model in sUED,” arXiv:0811.0387 [hep-ph].

P. J. Fox and E. Poppitz, “Leptophilic Dark Matter,” arXiv:0811.0399 [hep-ph].

D. Hooper and K. M. Zurek, “The PAMELA and ATIC Signals From Kaluza-Klein Dark Matter,” arXiv:0902.0593 [hep-ph].

H. S. Goh, L. J. Hall and P. Kumar, “The Leptonic Higgs as a Messenger of Dark Matter,” JHEP **0905**, 097 (2009) [arXiv:0902.0814 [hep-ph]].

C. Cheung, J. T. Ruderman, L. T. Wang and I. Yavin, arXiv:0902.3246 [hep-ph].

A. Ibarra, A. Ringwald, D. Tran and C. Weniger, “Cosmic Rays from Leptophilic Dark Matter Decay via Kinetic Mixing,” JCAP **0908**, 017 (2009) [arXiv:0903.3625 [hep-ph]].

K. Kohri, J. McDonald and N. Sahu, “Cosmic Ray Anomalies and Dark Matter Annihilation to Muons via a Higgs Portal Hidden Sector,” arXiv:0905.1312 [hep-ph].

D. Hooper and T. M. P. Tait, “Extended MSSM Neutralinos as the Source of the PAMELA Positron Excess,” arXiv:0906.0362 [hep-ph].

P. H. Gu, U. Sarkar and X. Zhang, “Visible and Dark Matter Genesis and Cosmic Positron/Electron Excesses,” arXiv:0906.3103 [hep-ph].

P. H. Gu, H. J. He, U. Sarkar and X. Zhang, “Double Type-II Seesaw, Baryon Asymmetry and Dark Matter for Cosmic $e^{\pm}$ Excesses,” arXiv:0906.0442 [hep-ph].

K. Kohri, A. Mazumdar, N. Sahu and P. Stephens, “Probing Unified Origin of Dark Matter and Baryon Asymmetry at PAMELA/Fermi,” arXiv:0907.0622 [hep-ph].

[28] D. Hooper and L. T. Wang, “Evidence for axino dark matter in the galactic bulge,” Phys. Rev. D **70**, 063506 (2004) [arXiv:hep-ph/0402220].

C. Picciotto and M. Pospelov, “Unstable relics as a source of galactic positrons,” Phys. Lett. B **605**, 15 (2005) [arXiv:hep-ph/0402178].

C. R. Chen, F. Takahashi and T. T. Yanagida, “High-energy Cosmic-Ray Positrons from Hidden-Gauge-Boson Dark Matter,” Phys. Lett. B **673**, 255 (2009) [arXiv:0811.0477 [hep-ph]].

C. R. Chen, M. M. Nojiri, F. Takahashi and T. T. Yanagida, “Decaying Hidden Gauge Boson and the PAMELA and ATIC/PPB-BETS Anomalies,” arXiv:0811.3357 [astro-ph].

E. Nardi, F. Sannino and A. Strumia, “Decaying Dark Matter can explain the electron/positron excesses,” JCAP **0901**, 043 (2009) [arXiv:0811.4153 [hep-ph]].

S. C. Park and J. Shu, “Split-UED and Dark Matter,” Phys. Rev. D **79**, 091702 (2009) [arXiv:0901.0720 [hep-ph]].

C. R. Chen, M. M. Nojiri, S. C. Park, J. Shu and M. Takeuchi, “Dark matter and collider phenomenology of split-UED,” arXiv:0903.1971 [hep-ph].

S. L. Chen, R. N. Mohapatra, S. Nussinov and Y. Zhang, “R-Parity Breaking via Type II Seesaw, Decaying Gravitino Dark Matter and PAMELA Positron Excess,” Phys. Lett. B **677**, 311 (2009) [arXiv:0903.2562 [hep-ph]].

A. Arvanitaki, S. Dimopoulos, S. Dubovsky, P. W. Graham, R. Harnik and S. Rajendran, “Decaying Dark Matter as a Probe of Unification and TeV Spectroscopy,” arXiv:0904.2789 [hep-ph].

H. Murayama and J. Shu, “Topological Dark Matter,” arXiv:0905.1720 [hep-ph].

N. Okada and T. Yamada, “The PAMELA and Fermi signals from long-lived Kaluza-Klein dark matter,” arXiv:0905.2801 [hep-ph].

J. Mardon, Y. Nomura and J. Thaler, “Cosmic Signals from the Hidden Sector,” arXiv:0905.3749 [hep-ph].

K. Ishiwata, S. Matsumoto and T. Moroi, “Cosmic Gamma-ray from Inverse Compton Process in Unstable Dark Matter Scenario,” arXiv:0905.4593 [astro-ph.CO].

A. Ibarra, D. Tran and C. Weniger, “Decaying Dark Matter in Light of the PAMELA and Fermi LAT Data,” arXiv:0906.1571 [hep-ph].

M. R. Buckley, K. Freese, D. Hooper, D. Spolyar and H. Murayama, “High-Energy Neutrino Signatures of Dark Matter Decaying into Leptons,” arXiv:0907.2385 [astro-ph.HE].

C. R. Chen, M. M. Nojiri, S. C. Park and J. Shu, “Kaluza-Klein Dark Matter After Fermi,” arXiv:0908.4317 [hep-ph].

[29] B. Katz, K. Blum and E. Waxman, “What can we really learn from positron flux ’anomalies’?,” arXiv:0907.1686 [astro-ph.HE].

[30] R. E. Lingenfelter, J. C. Higdon and R. E. Rothschild, “Is There a Dark Matter Signal in the Galactic Positron Annihilation Radiation?,” Phys. Rev. Lett. **103**, 031301 (2009) [arXiv:0904.1025 [astro-ph.HE]]; “The Galactic Positron Annihilation Radiation & The Propagation of Positrons in the Interstellar Medium,” Astrophys. J. **698**, 350 (2009) [arXiv:0711.3008 [astro-ph]].

[31] D. Hooper, P. Blasi and P. D. Serpico, “Pulsars as the Sources of High Energy Cosmic Ray Positrons,” JCAP **0901**, 025 (2009) [arXiv:0810.1527 [astro-ph]].

H. Yuksel, M. D. Kistler and T. Stanev, “TeV Gamma Rays from Geminga and the Origin of the GeV Positron Excess,” arXiv:0810.2784 [astro-ph].

P. D. Serpico, “On the possible causes of a rise with energy of the cosmic ray positron fraction,” Phys. Rev. D **79**, 021302 (2009) [arXiv:0810.4846 [hep-ph]].

I. Buesching, O. C. de Jager, M. S. Potgieter and C. Venter, “A Cosmic Ray Positron Anisotropy due to Two Middle-Aged, Nearby Pulsars?,” arXiv:0804.0220 [astro-ph].

S. Profumo, “Dissecting Pamela (and ATIC) with Oc-

cam's Razor: existing, well-known Pulsars naturally account for the 'anomalous' Cosmic-Ray Electron and Positron Data," arXiv:0812.4457 [astro-ph].
V. Barger, Y. Gao, W. Y. Keung, D. Marfatia and G. Shaughnessy, "Dark matter and pulsar signals for Fermi LAT, PAMELA, ATIC, HESS and WMAP data," arXiv:0904.2001 [hep-ph].
D. Grasso *et al.* [FERMI-LAT Collaboration], "On possible interpretations of the high energy electron-positron spectrum measured by the Fermi Large Area Telescope," arXiv:0905.0636 [astro-ph.HE].
D. Grasso and f. L. collaboration, "Possible Interpretations of the High Energy Cosmic Ray Electron Spectrum measured with the Fermi Space Telescope," arXiv:0907.0373 [astro-ph.HE].

[32] J. Hisano, M. Kawasaki, K. Kohri and K. Nakayama, "Neutrino Signals from Annihilating/Decaying Dark Matter in the Light of Recent Measurements of Cosmic Ray Electron/Positron Fluxes," arXiv:0812.0219 [hep-ph].

[33] L. Bergstrom, G. Bertone, T. Bringmann, J. Edsjo and M. Taoso, "Gamma-ray and Radio Constraints of High Positron Rate Dark Matter Models Annihilating into New Light Particles," arXiv:0812.3895 [astro-ph].

[34] E. Borriello, A. Cuoco and G. Miele, "Secondary radiation from the Pamela/ATIC excess and relevance for Fermi," arXiv:0903.1852 [astro-ph.GA].

[35] M. Cirelli and P. Panci, "Inverse Compton constraints on the Dark Matter e+e- excesses," arXiv:0904.3830 [astro-ph.CO].

[36] F. Y. Cyr-Racine, S. Profumo and K. Sigurdson, arXiv:0904.3933 [astro-ph.CO].

[37] M. Regis and P. Ullio, "Testing the Dark Matter Interpretation of the PAMELA Excess through Measurements of the Galactic Diffuse Emission," arXiv:0904.4645 [astro-ph.GA].

[38] A. Pinzke, C. Pfrommer and L. Bergstrom, "Gamma-rays from dark matter annihilations strongly constrain the substructure in halos," arXiv:0905.1948 [astro-ph.HE].

[39] J. Hisano, K. Nakayama and M. J. S. Yang, "Upward muon signals at neutrino detectors as a probe of dark matter properties," arXiv:0905.2075 [hep-ph].

[40] D. Spolyar, M. Buckley, K. Freese, D. Hooper and H. Murayama, "High Energy Neutrinos As A Test of Leptophilic Dark Matter," arXiv:0905.4764 [astro-ph.CO].

[41] S. Profumo and T. E. Jeltema, "Extragalactic Inverse Compton Light from Dark Matter Annihilation and the Pamela Positron Excess," arXiv:0906.0001 [astro-ph.CO].

[42] T. R. Slatyer, N. Padmanabhan and D. P. Finkbeiner, "CMB Constraints on WIMP Annihilation: Energy Absorption During the Recombination Epoch," arXiv:0906.1197 [astro-ph.CO].

[43] A. V. Belikov and D. Hooper, "The Contribution Of Inverse Compton Scattering To The Diffuse Extragalactic Gamma-Ray Background From Annihilating Dark Matter," arXiv:0906.2251 [astro-ph.CO].

[44] G. Hütsi, A. Hektor and M. Raidal, "Constraints on leptonically annihilating Dark Matter from reionization and extragalactic gamma background," arXiv:0906.4550 [astro-ph.CO].

[45] M. Kuhlen, P. Madau and J. Silk, "Exploring Dark Matter with Milky Way substructure," arXiv:0907.0005 [astro-ph.GA].

[46] M. Cirelli, F. Iocco and P. Panci, "Constraints on Dark Matter annihilations from reionization and heating of the intergalactic gas," arXiv:0907.0719 [astro-ph.CO].

[47] I. Cholis, G. Dobler, D. P. Finkbeiner, L. Goodenough, T. R. Slatyer and N. Weiner, "The Fermi gamma-ray spectrum of the inner galaxy: Implications for annihilating dark matter," arXiv:0907.3953 [astro-ph.HE].

[48] T. Kanzaki, M. Kawasaki and K. Nakayama, "Effects of Dark Matter Annihilation on the Cosmic Microwave Background," arXiv:0907.3985 [astro-ph.CO].

[49] J. Hisano, S. Matsumoto and M. M. Nojiri, "Explosive dark matter annihilation," Phys. Rev. Lett. **92**, 031303 (2004) [arXiv:hep-ph/0307216].
J. Hisano, S. Matsumoto, M. M. Nojiri and O. Saito, "Non-perturbative effect on dark matter annihilation and gamma ray signature from galactic center," Phys. Rev. D **71**, 063528 (2005) [arXiv:hep-ph/0412403]
J. March-Russell, S. M. West, D. Cumberbatch and D. Hooper, "Heavy Dark Matter Through the Higgs Portal," JHEP **0807**, 058 (2008) [arXiv:0801.3440 [hep-ph]].
M. Lattanzi and J. I. Silk, "Can the WIMP annihilation boost factor be boosted by the Sommerfeld enhancement?," arXiv:0812.0360 [astro-ph].
J. D. March-Russell and S. M. West, "WIMPonium and Boost Factors for Indirect Dark Matter Detection," Phys. Lett. B **676**, 133 (2009) [arXiv:0812.0559 [astro-ph]].

[50] F. Chen, J. M. Cline and A. R. Frey, "A new twist on excited dark matter: implications for INTEGRAL, PAMELA/ATIC/PPB-BETS, DAMA," Phys. Rev. D **79**, 063530 (2009) arXiv:0901.4327 [hep-ph].

[51] Y. Cui, D. E. Morrissey, D. Poland and L. Randall, "Candidates for Inelastic Dark Matter," JHEP **0905**, 076 (2009) [arXiv:0901.0557 [hep-ph]].
D. P. Finkbeiner, T. Lin and N. Weiner, "Inelastic Dark Matter and DAMA/LIBRA: An Experimentum Crucis," arXiv:0906.0002 [astro-ph.CO].
J. Kopp, V. Niro, T. Schwetz and J. Zupan, "DAMA/LIBRA and leptonically interacting Dark Matter," arXiv:0907.3159 [hep-ph].

[52] D. B. Cline, W. Ooi and H. Wang, "A Constraint on Inelastic Dark Matter Signal using ZEPLIN-II Results," arXiv:0906.4119 [astro-ph.CO].
K. Schmidt-Hoberg and M. W. Winkler, "Improved Constraints on Inelastic Dark Matter," arXiv:0907.3940 [astro-ph.CO].

[53] B. Batell, M. Pospelov and A. Ritz, "Direct Detection of Multi-component Secluded WIMPs," arXiv:0903.3396 [hep-ph].

[54] W. Wang *et al.*, "Spectral and intensity variations of Galactic ^{26}Al emission," arXiv:0902.0211 [astro-ph.HE].

[55] T. P. Cheng, "Chiral Symmetry And The Higgs Nucleon Coupling," Phys. Rev. D **38**, 2869 (1988).

[56] http://wwwlapp.in2p3.fr/lapth/micromegas/

[57] P. Grajek, G. Kane, D. Phalen, A. Pierce and S. Watson, "Is the PAMELA Positron Excess Winos?," arXiv:0812.4555 [hep-ph];
G. Kane, R. Lu and S. Watson, "PAMELA Satellite Data as a Signal of Non-Thermal Wino LSP Dark Matter," arXiv:0906.4765 [astro-ph.HE].

[58] D. P. Finkbeiner, T. R. Slatyer, N. Weiner and I. Yavin, "PAMELA, DAMA, INTEGRAL and Signatures of Metastable Excited WIMPs," arXiv:0903.1037 [hep-ph].

[59] D. G. E. Walker, "Dark Matter Stabilization Symmetries from Spontaneous Symmetry Breaking,"

arXiv:0907.3146 [hep-ph]; "Dark Matter Stabilization Symmetries and Long-Lived Particles at the Large Hadron Collider," arXiv:0907.3142 [hep-ph].

[60] See eq. (22.1,22.6) of C. Amsler et al., Physics Letters B667, 1 (2008), http://pdg.lbl.gov/2008/reviews/rpp2008-rev-dark-matter.pdf

[61] B. Robertson and A. Zentner, "Dark Matter Annihilation Rates with Velocity-Dependent Annihilation Cross Sections," Phys. Rev. D **79**, 083525 (2009) arXiv:0902.0362 [astro-ph.CO].

[62] J. Bovy, "Substructure Boosts to Dark Matter Annihilation from Sommerfeld Enhancement," arXiv:0903.0413 [astro-ph.HE].

[63] J. Diemand, M. Kuhlen, P. Madau, M. Zemp, B. Moore, D. Potter and J. Stadel, "Clumps and streams in the local dark matter distribution," Nature 454 (2008) 735-738; arXiv:0805.1244 [astro-ph].

[64] E. Romano-Diaz, I. Shlosman, Y. Hoffman and C. Heller, "Erasing Dark Matter Cusps in Cosmological Galactic Halos with Baryons," arXiv:0808.0195 [astro-ph].

[65] M. G. Abadi, J. F. Navarro, M. Fardal, A. Babul and M. Steinmetz, "Galaxy-Induced Transformation of Dark Matter Halos," arXiv:0902.2477 [astro-ph.GA].

[66] J.F. Navarro, private communication

[67] X. J. Bi, R. Brandenberger, P. Gondolo, T. Li, Q. Yuan and X. Zhang, "Non-Thermal Production of WIMPs, Cosmic $e^{\pm}$ Excesses and γ-rays from the Galactic Center," arXiv:0905.1253 [hep-ph].

[68] M. Pospelov and A. Ritz, "The galactic 511-keV line from electroweak scale WIMPs," Phys. Lett. B **651**, 208 (2007) [arXiv:hep-ph/0703128].

[69] F. Chen, J.M. Cline, A. Fradette, A. Frey, C. Rabideau, work in progress

[70] E.W. Kolb and M.S. Turner, "The Early universe," Front. Phys. **69** (1990) 1.

[71] J. D. Bjorken, R. Essig, P. Schuster and N. Toro, "New Fixed-Target Experiments to Search for Dark Gauge Forces," arXiv:0906.0580 [hep-ph].

[72] M. Pospelov, "Secluded U(1) below the weak scale," arXiv:0811.1030 [hep-ph].

[73] B. Batell, M. Pospelov and A. Ritz, "Exploring Portals to a Hidden Sector Through Fixed Targets," arXiv:0906.5614 [hep-ph].

[74] D. P. Finkbeiner, T. Lin and N. Weiner, "Inelastic Dark Matter and DAMA/LIBRA: An Experimentum Crucis," arXiv:0906.0002 [astro-ph.CO].

[75] M. Baumgart, C. Cheung, J. T. Ruderman, L. T. Wang and I. Yavin, "Non-Abelian Dark Sectors and Their Collider Signatures," JHEP **0904**, 014 (2009) [arXiv:0901.0283 [hep-ph]].

[76] M. Pospelov, A. Ritz and M. B. Voloshin, "Bosonic super-WIMPs as keV-scale dark matter," Phys. Rev. D **78**, 115012 (2008) [arXiv:0807.3279 [hep-ph]].